The parametrization of the planetary boundary layer
May 1992

By **Anton Beljaars**

European Centre for Medium-Range Weather Forecasts

Table of contents

1. INTRODUCTION

1.1 The planetary boundary layer

The planetary boundary layer (PBL) is the region of the atmosphere near the surface where the influence of the surface is felt through turbulent exchange of momentum, heat and moisture. The equations which describe the large-scale evolution of the atmosphere do not take into account the interaction with the surface. The turbulent motion responsible for this interaction is small-scale and totally sub-grid and therefore needs to be parametrized.

The transition region between the surface and the free atmosphere, where vertical diffusion due to turbulent motion takes place, varies in depth. The PBL can be as shallow as 100 m during night over land and go up to a few thousand metres when the atmosphere is heated from the surface. The PBL parametrization determines together with the surface parametrization the surface fluxes and redistributes the surface fluxes over the boundary layer depth. Boundary layer processes are relatively quick; the PBL responds to its forcing within a few hours which is fast compared to the time scale of the large-scale evolution of the atmosphere, in other words: the PBL is always in quasi-equilibrium with the large-scale forcing.

1.2 Importance of the PBL in large-scale models

A number of reasons exists to have a realistic representation of the boundary layer in a large scale model:
- The large-scale budgets of momentum heat and moisture are considerably affected by the surface fluxes on time scales of a few days.
- Model variables in the boundary layer are important model products.
- The boundary layer interacts with other processes e.g. clouds and convection.

The importance of the surface fluxes can be illustrated by estimating the recycle time of the different quantities on the basis of typical values of the surface fluxes. The numbers in Table 1 have been derived from a typical run with the ECMWF model or are simply order of magnitudes estimations.

Already from these very crude estimates it can be seen that the surface fluxes play an important role in forecasting for the medium range. It is obvious that the surface fluxes are crucial for the "climate" of the model. With regard to the momentum budget it should be noted that the Ekman spin-down time has to be considered as the relevant time scale because it is an efficient mechanism for spinning down vorticity in the entire atmosphere by frictional stress in the PBL only.

The second important reason to have a PBL scheme in a large-scale model is that forecast products are needed near the surface. The temperature and wind at standard observation height (2 m and 10 m for temperature and wind respectively) are obvious products. It is important to realize that the PBL scheme together with the land surface and radiation scheme introduces the diurnal pattern in the surface fields. Also the analysed and forecasted fields of surface fluxes (momentum, heat and moisture) are becoming more and more important as input and verification for wave models, air pollution models and climate models.

TABLE 1. GLOBAL BUDGETS (ORDER OF MAGNITUDE ESTIMATES)

Budget	Total	Surface flux	Recycle time
Water	7×10^7 J m^{-2}	80 W m^{-2}	10 days

TABLE 1. GLOBAL BUDGETS (ORDER OF MAGNITUDE ESTIMATES)

Budget	Total	Surface flux	Recycle time
Internal + potential energy	4×10^9 J m^{-2} (0.5% available)	30 W m^{-2}	8 days
Kinetic energy	2×10^6 J m^{-2}	2 W m^{-2}	10 days
Momentum	2×10^5 kg m s^{-1}	0.1 N m^{-2}	25 days (Eckman spin-down time: 4 days

Finally it has to be realized that other processes can not be parametrized properly without having a PBL scheme. Boundary layer clouds are an obvious example, but also convection schemes often use surface fluxes of moisture in their closure.

1.3 Recommended literature

General textbook and introductory review on most aspects of the PBL:

Stull, R.B. (1988): *An introduction to boundary layer meteorology*. Kluwer publishers.

Introduction to turbulence:

Tennekes, H. and Lumley, J.L. (1972): *A first course in turbulence*. MIT press.

Atmospheric turbulence:

Nieuwstadt, F.T.M. and Van Dop, H. (eds. 1982): *Atmospheric turbulence and air pollution modelling*. Reidel publishers.

Haugen, D.A. (ed. 1973): *Workshop on micro meteorology*. Am. Meteor. Soc.

Monin, A.S. and Yaglom, A.M. (1971): *Statistical fluid dynamics*. Vol I, MIT press.

Panofsky, H.A. and Dutton, J.A. (1984): *Atmospheric turbulence: Models and methods for engineering applications*. John Wiley and sons.

Surface fluxes:

Oke, T.R. (1978): *Boundary layer climates*. Halsted press.

Brutsaert, W. (1982): *Evaporation into the atmosphere*. Reidel publishers.

1.4 General characteristics of the planetary boundary layer

Turbulence

The diffusive processes in the atmospheric boundary are dominated by turbulence. The molecular diffusion can in general be neglected except in a shallow layer (a few mm only) near the surface. The time scale of the turbulent motion ranges from a few seconds for the small eddies to about half an hour for the biggest eddies (see Fig. 1). The length scales vary from millimetres for the dissipative fluctuations to a few hundred metres for the eddies in the bulk of the boundary layer. The latter ones dominate the diffusive properties of the turbulent boundary layer. It is clear that these scales cannot be resolved by large-scale models and need to be parametrized.
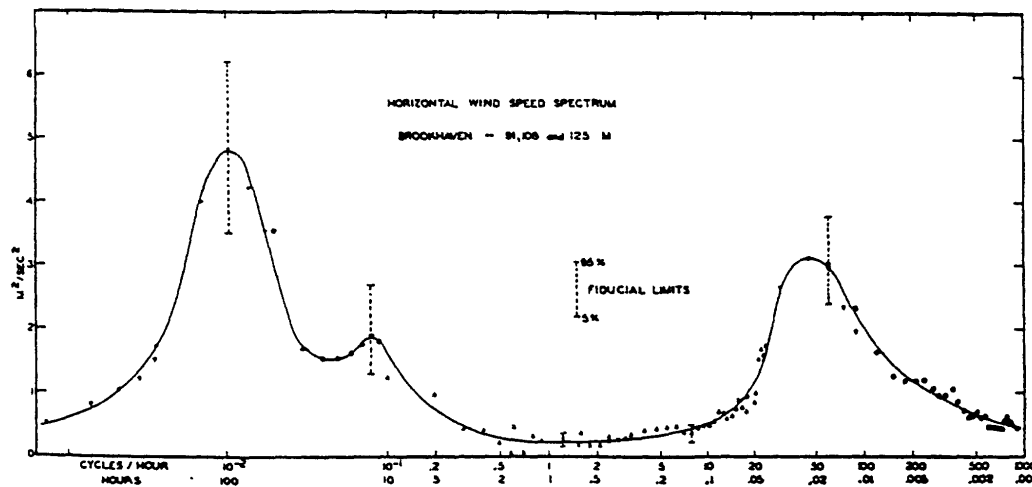
Figure 1. Spectrum of the horizontal wind velocity after Van Der Hoven (1957). Some experimental points are shown.

Stability

The structure of the atmospheric boundary layer is influenced by the underlying surface and by the stability of the PBL (see Fig. 2).

The surface roughness determines to a certain extent the amount of turbulence production, the surface stress and the shape of the wind profile. Stability influences the structure of turbulence. In an unstably stratified PBL (e.g. during day-time over land with an upward heat flux from the surface) the turbulence production is enhanced and the exchange is intensified resulting in a more uniform distribution of momentum, potential temperature and specific humidity. In a stably stratified boundary layer (e.g. during night-time over land) the turbulence produced by shear is suppressed by the stratification resulting in a weak exchange and a weak coupling with the surface. The qualitative impact of these aspect is illustrated in Fig. 2

Diurnal pattern

The typical evolution of the PBL over land is illustrated in Fig. 3 for a 24 hour interval. During daytime, with an upward heat flux from the surface, the turbulent mixing is very strong, resulting in approximately uniform profiles of potential temperature and wind over the bulk of the boundary layer. The unstable boundary layer is therefore often called "mixed layer". Near the surface we see a super adiabatic layer and a strong wind gradient. The top of the mixed layer is capped by an inversion which inhibits the turbulent motion (e.g. the rising thermals) to penetrate aloft. The inversion height rises quickly early in the morning an reaches a height of a few kilometres during daytime. When the heat flux from the surface changes sign at night the turbulence in the mixed layer dies out and a shallow stable layer near the surface develops. The nocturnal boundary layer has a height of typically 50 to 200 m dependent on wind speed and stability.
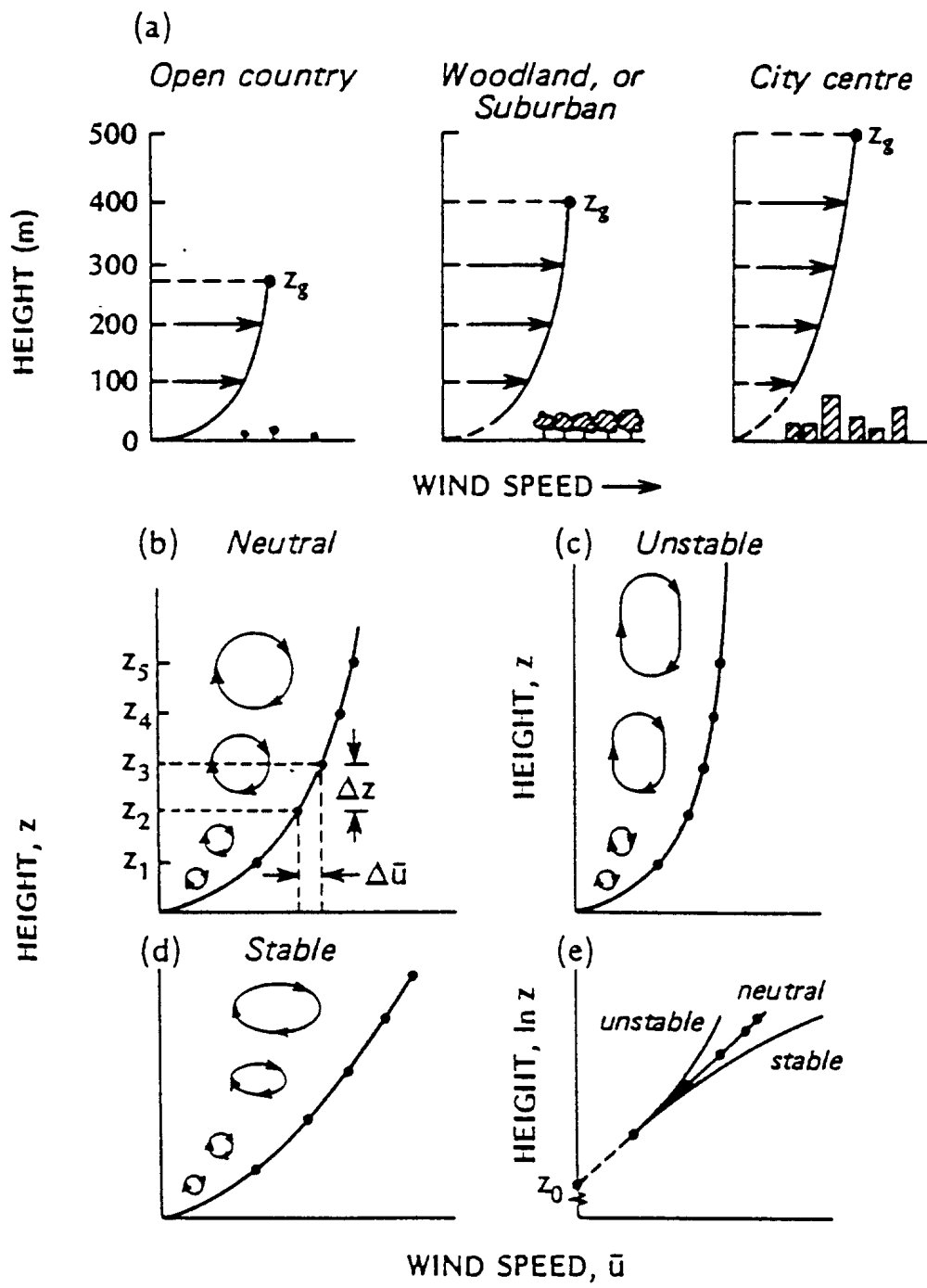
Figure 2. The wind speed profile near the ground including (a) the effect of terrain roughness, and (b) to (e) the effect of stability on profile shape end eddy structure. In (e) the profiles of (b) to (d) are re-plotted with a logarithmic height scale. (Fig. 2.10 from Oke, 1978).
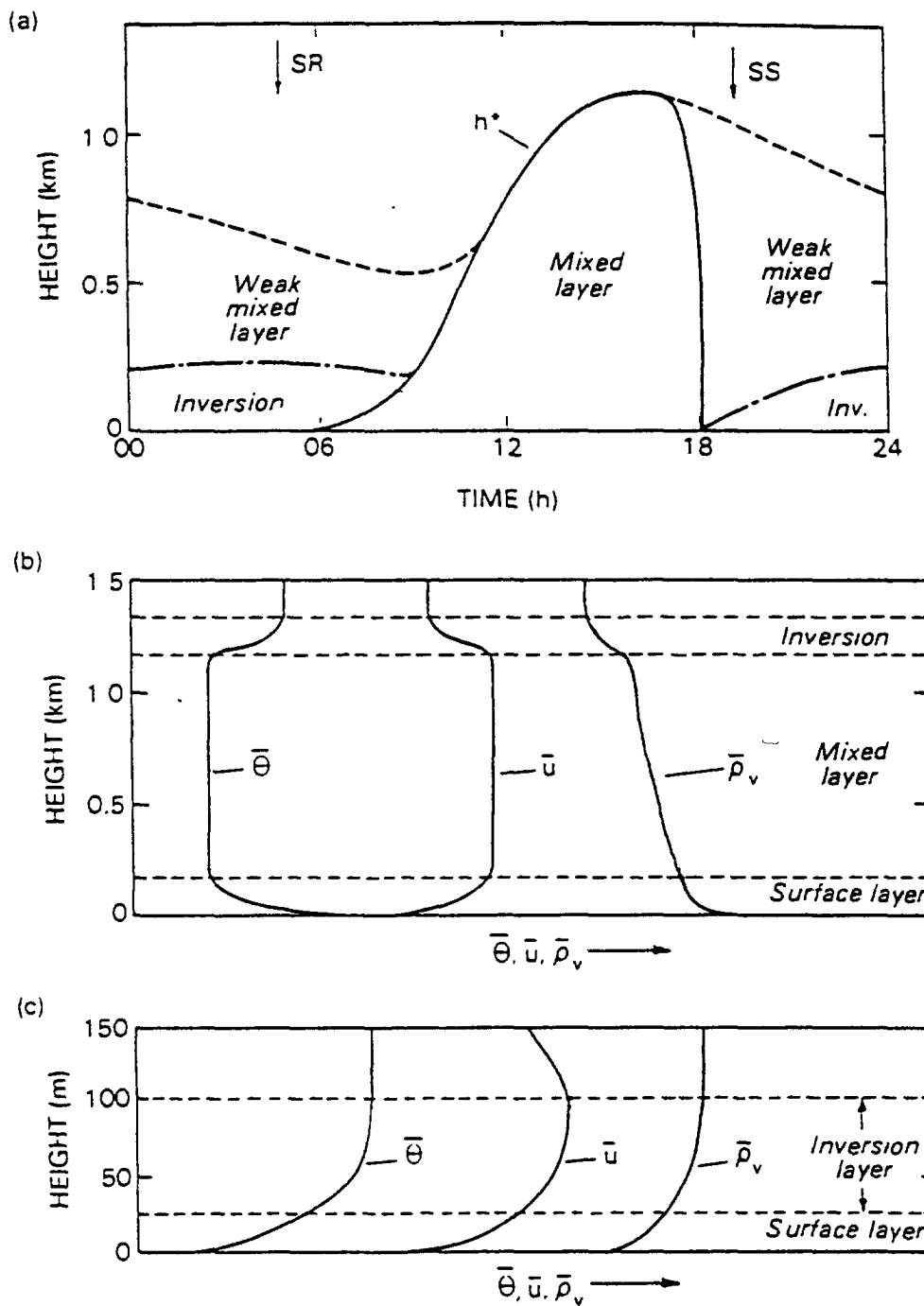
Figure 3. (a) Diurnal variation of the boundary layer on an "ideal" day. (b) Idealized mean profiles of potential temperature (θ), wind speed (U) and density (ρ_v) for the daytime convective boundary layer. (c) Same as (b) for nocturnal stable layer. The arrows indicate sunrise and sunset.

Surface fluxes
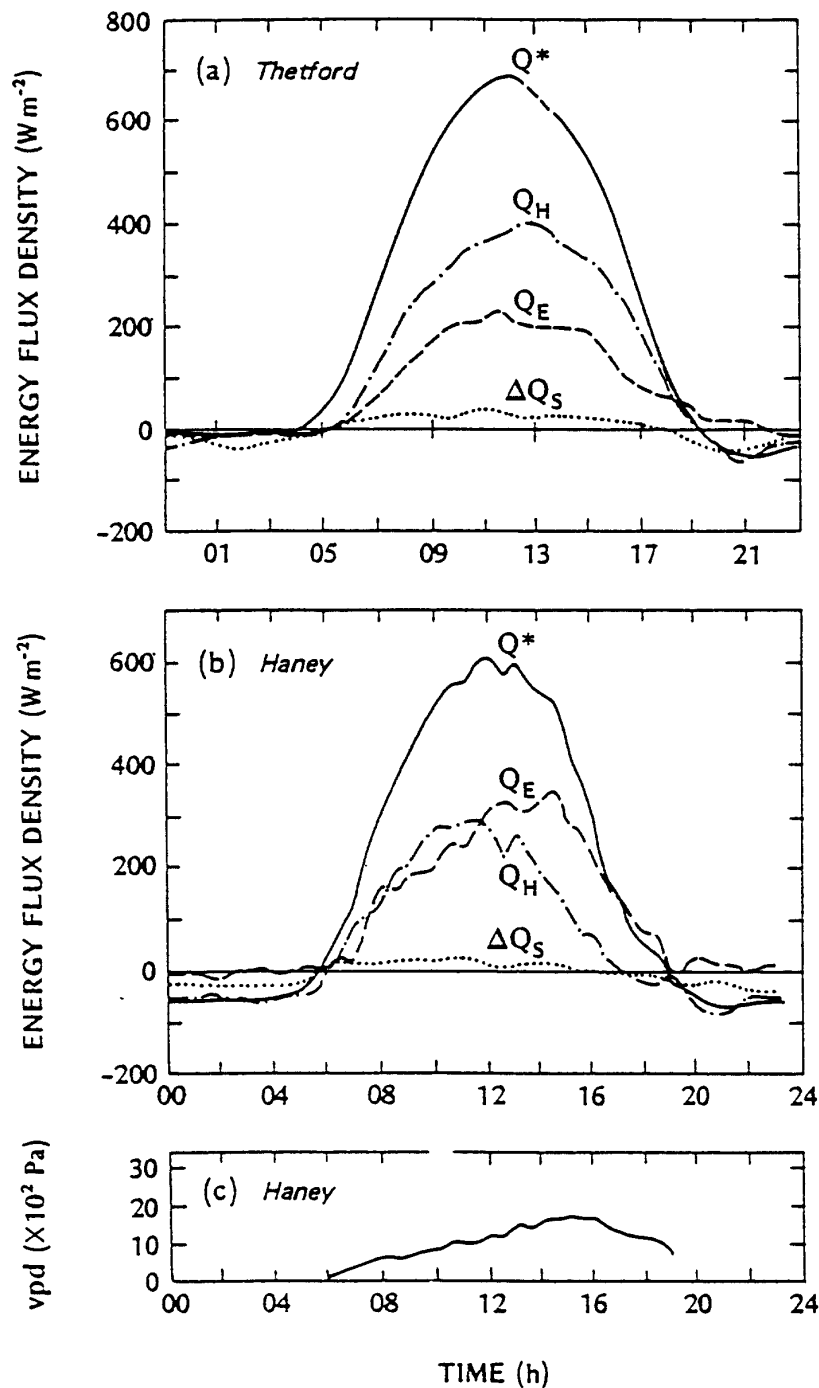
Figure 4. Diurnal energy balance of (a) a Scots and Corsican pine forest at Thetford (England) on 7 July 1971, and (b) a Douglas fir forest at Haney (B.C. Canada) on 10 July 1970, including (c) the atmospheric vapour pressure deficit. In these figures Q_* represents net radiation, Q_H the sensible heat flux, Q_E the latent heat flux and ΔQ_s the soil heat flux. (Fig. 4.24 from Oke 1978).

The surface fluxes of momentum, heat an moisture are of crucial importance to the model as they affect the climate

of the model, the model performance in the medium range and play an integral role in a number of parametrizations. The diurnal pattern of the PBL over land is mainly forced by the energy budget at the surface through the diurnal evolution of the net radiation at the surface as illustrated in Fig. 4 . During daytime the net radiation is partitioned between the heat flux into the ground, the sensible heat flux into the atmosphere and the latent heat of evaporation. The ground heat flux is generally smaller than 10% of the net radiation during daytime. The partitioning of available net radiation between sensible and latent heat is part of the land surface parametrization scheme. The fluxes are much smaller during night-time and are much less important for the atmospheric budgets but equally relevant for the prediction of boundary layer parameters.

The boundary layer over sea does not have a distinct diurnal pattern but can be stable and unstable dependent of the air type that is advected relative to the sea surface temperature. Strong cold air advection over a relatively warm sea can lead to extremely high fluxes of sensible and latent heat into the atmosphere. Warm air advection over a cold sea leads to a stable PBL but does occur less frequently.

It is important to realize that the thermodynamic surface boundary conditions over sea are very different from those over land. Over sea the temperature and specific humidity are specified and kept constant during the forecast. Over land the surface boundary condition for temperature and moisture are nearly flux boundary conditions, because of the constraint imposed by the surface energy budget. In the latter case, the fluxes are determined by the net radiation at the surface. This means that the total energy input into the atmosphere (sensible + latent heat) is not so much determined by the flow or by the PBL parametrization but by the net radiation at the surface. The sea however, is, with its fixed SST boundary condition, an infinite source of energy to the model. The specification of the PBL exchange with the sea surface is therefore extremely critical. Beljaars and Miller (1991) give an example of model sensitivity to the parametrization of surface fluxes over tropical oceans.

PBL clouds

Cumulus clouds, stratocumulus clouds and fog are very much part of the boundary layer dynamics and interact strongly with radiation.

1.5 Conserved quantities and static stability

To describe vertical diffusion by turbulent motion we have to select variables that are conserved for adiabatic processes. In the hydrostatic approximation both potential temperature θ and dry static energy are conserved for dry adiabatic ascent or descent. They are defined as

$$\theta = T(p_0/p)^{R/c_p} \approx T(p_0/p)^{0.286} \tag{1}$$

$$s = c_p T + gz \tag{2}$$

When moist processes are considered as well it is necessary to use liquid water potential temperature θ_l or the liquid water static energy s_l and total water content q_t:

$$\theta_l = \theta - \left(\frac{L_{vap}\theta}{c_p T}\right)q_1 \tag{3}$$

$$s_l = c_p T + gz - L_{vap}q_1 \tag{4}$$

$$q_t = q + q_1 \tag{5}$$

The static stability is determined by the density of a fluid parcel moved adiabatically to a reference height in comparison with the density of the surrounding fluid. The virtual potential temperature θ_v and the virtual dry static energy are often used for this purpose:

$$\theta_v = \theta\left[1 + \left(\frac{R_v}{R} - 1\right)q - q_1\right] = \theta\{1 + 0.61q - q_1\} \tag{6}$$

$$s_v = c_p T\{1 + 0.61q - q_1\} + gz \tag{7}$$

1.6 Basic equations

To illustrate the closure problem we derive the Reynolds equations for momentum, starting from the three momentum equations for incompressible flow in a rectangular coordinate system with z perpendicular to the earth surface:

$$
\begin{aligned}
\frac{\partial u}{\partial t} + u\frac{\partial u}{\partial x} + v\frac{\partial u}{\partial y} + w\frac{\partial u}{\partial z} - fv &= -\frac{1}{\rho}\frac{\partial p}{\partial x} + \nu\nabla^2 u \\
\frac{\partial v}{\partial t} + u\frac{\partial v}{\partial x} + v\frac{\partial v}{\partial y} + w\frac{\partial v}{\partial z} + fu &= -\frac{1}{\rho}\frac{\partial p}{\partial y} + \nu\nabla^2 v \\
\frac{\partial w}{\partial t} + u\frac{\partial w}{\partial x} + v\frac{\partial w}{\partial y} + w\frac{\partial w}{\partial z} &= -\frac{1}{\rho}\frac{\partial p}{\partial z} + \nu\nabla w - g
\end{aligned}
\tag{8}
$$

$$\frac{\partial u}{\partial x} + \frac{\partial v}{\partial y} + \frac{\partial w}{\partial z} = 0 \tag{9}$$

Decomposition of each variable into a mean part and a fluctuating (turbulent) part:

$$
\begin{aligned}
u &= U + u' \quad , \quad \rho = \rho_0 + \rho' \quad , \\
v &= V + v' \quad , \quad p = P + p' \quad , \\
w &= W + w'
\end{aligned}
\tag{10}
$$

After averaging, application of the Boussinesq approximation (retain density fluctuations in the buoyancy terms only) and applying the hydrostatic approximation:

$$
\begin{aligned}
\frac{\partial U}{\partial t} + U\frac{\partial U}{\partial x} + V\frac{\partial U}{\partial y} + W\frac{\partial U}{\partial z} - fV &= -\frac{1}{\rho_0}\frac{\partial P}{\partial x} + \nu\nabla^2 U - \frac{\partial}{\partial x}\overline{u'u'} - \frac{\partial}{\partial y}\overline{u'v'} - \frac{\partial}{\partial z}\overline{u'w'} \\
\frac{\partial V}{\partial t} + U\frac{\partial V}{\partial x} + V\frac{\partial V}{\partial y} + W\frac{\partial V}{\partial z} + fU &= -\frac{1}{\rho_0}\frac{\partial P}{\partial y} + \nu\nabla^2 V - \frac{\partial}{\partial x}\overline{u'v'} - \frac{\partial}{\partial y}\overline{v'v'} - \frac{\partial}{\partial z}\overline{v'w'} \\
g &= -\frac{1}{\rho_0}\frac{\partial P}{\partial z}
\end{aligned}
\tag{11}
$$

$$\frac{\partial U}{\partial x} + \frac{\partial V}{\partial y} + \frac{\partial W}{\partial z} = 0 \tag{12}$$

Further simplifications are obtained by neglecting viscous effects for large Reynolds numbers ($UL/\nu \gg 1$, where L is a length scale) and by assuming that the x, y-scales are much larger than the z-scales (boundary layer approximation):

$$\frac{\partial U}{\partial t} + U\frac{\partial U}{\partial x} + V\frac{\partial U}{\partial y} + W\frac{\partial U}{\partial z} - fV = -\frac{1}{\rho_0}\frac{\partial P}{\partial x} - \frac{\partial \overline{u'w'}}{\partial z}$$

$$\frac{\partial V}{\partial t} + U\frac{\partial V}{\partial x} + V\frac{\partial V}{\partial y} + W\frac{\partial V}{\partial z} + fU = -\frac{1}{\rho_0}\frac{\partial P}{\partial y} - \frac{\partial \overline{v'w'}}{\partial z} \tag{13}$$

$$g = -\frac{1}{\rho_0}\frac{\partial P}{\partial z}$$

These equations describe the horizontal momentum budget of the resolved flow and have extra terms due to the Reynolds decomposition and averaging procedure. The terms $\overline{u'w'}$ and $\overline{v'w'}$ are known as the Reynolds stresses and represent vertical transport of horizontal momentum by unresolved turbulent motion. These are the terms that need to be parametrized. Similar equations exist for potential temperature and specific humidity.

An equation that is important in some parametrization schemes and gives insight in the dynamics of turbulence is the equation for turbulent kinetic energy. To derive it, the equations for the fluctuating quantities are taken by subtracting the equations for mean momentum from the equations for total momentum. The kinetic energy of the fluctuations is obtained by multiplying the equations for the different components by the velocity fluctuation itself and by adding the three equations for the three components. The result is: $\overline{E'w'}$

$$E = \frac{1}{2}(\overline{u'^2} + \overline{v'^2} + \overline{w'^2}) \tag{14}$$

$$\frac{\partial E}{\partial t} + U\frac{\partial E}{\partial x} + V\frac{\partial E}{\partial y} + W\frac{\partial E}{\partial z} = \underset{\text{I}}{-\overline{u'w'}\frac{\partial U}{\partial z}} \quad \underset{\text{I}}{-\overline{v'w'}\frac{\partial V}{\partial z}} \quad \underset{\text{II}}{-\frac{g}{\rho_0}\overline{w'\rho'}}$$

$$+ \underset{\text{III}}{\frac{\partial}{\partial z}\Big(\overline{E'w'}} \quad \underset{\text{IV}}{+ \frac{\overline{p'w'}}{\rho}\Big)} \quad \underset{\text{V}}{-\varepsilon} \tag{15}$$

The left hand side of this equation represents time dependence and advection. The right hand side has source, sink and transport terms. Terms I represent mechanical production of turbulence by wind shear and convert energy of the mean flow into turbulence. Term two is the production of turbulence by buoyancy and converts potential energy of the atmosphere to turbulence or vice versa. Terms III and IV are transport or turbulent diffusion terms because they equal zero when vertically integrated over the domain. They represent the vertical transport of turbulence energy by the turbulent fluctuations and the pressure fluctuations respectively. The last term (V) is the dissipation term which converts turbulence kinetic energy into heat by molecular friction at very small scales.

1.7 Ekman equation

To illustrate the mechanism of Ekman pumping we consider the following equations for the steady state boundary layer:

$$-f(V - V_{\text{G}}) = -\frac{\partial \overline{u'w'}}{\partial z}, \quad \text{where} \quad fV_{\text{G}} = \frac{1}{\rho_0}\frac{\partial P}{\partial x} \tag{16}$$

$$-f(U - U_{\text{G}}) = -\frac{\partial \overline{v'w'}}{\partial z}, \quad \text{where} \quad fU_{\text{G}} = -\frac{1}{\rho_0}\frac{\partial P}{\partial y} \tag{17}$$

For a simple closure with $\overline{u'w'} = -K\partial U/\partial z$, $\overline{v'w'} = -K\partial V/\partial z$ and constant K we rewrite the equations in complex notation:

$$\mathrm{i}f(U + \mathrm{i}V) - \mathrm{i}f(U_\mathrm{G} - \mathrm{i}V_\mathrm{G}) = K\frac{\partial^2}{\partial z^2}(U + \mathrm{i}V) \tag{18}$$
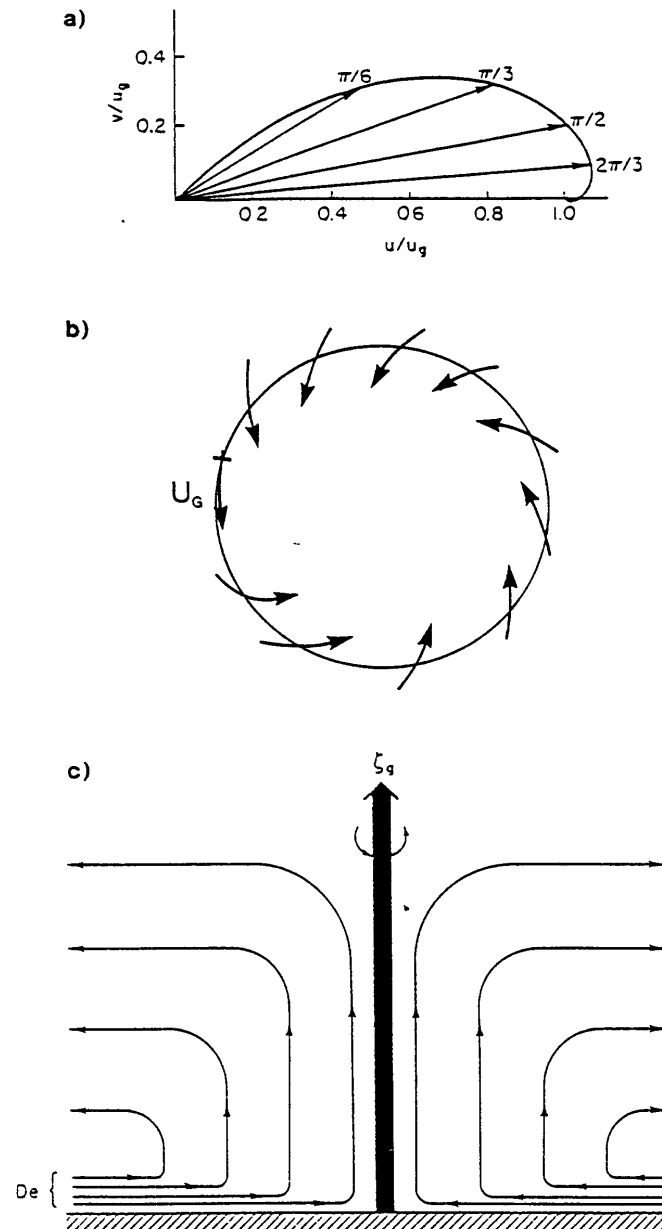

Figure 5. (a) Hodograph of Ekman spiral; the vectors indicate the increase of wind speed and its veering with height, (b) Illustration of the ageostrophic wind in the PBL of a cyclone, and (c) vertical velocity in cyclone due to Ekman pumping (Holton, 1979).

The solution with $U = V = 0$ at the surface and $U = U, V = V$ far away from the surface, reads:

$$(U + iV) \; = \; (U_G - iV_G) - (U_G - iV_G)\exp\left[\left(\frac{if}{K}\right)^{1/2}z\right] \tag{19}$$

The vertical velocity W_h at the top of the PBL is derived from the continuity equation by integration from the surface to boundary layer depth h, where h is large.

$$W_h = \int_0^h \left(-\frac{\partial U}{\partial x} - \frac{\partial V}{\partial y}\right)\mathrm{d}z \; = \; \frac{1}{f}\left(-\frac{\partial \overline{v'w'}}{\partial x} + \frac{\partial \overline{u'w'}}{\partial y}\right)$$

$$= \left(\frac{K}{2f}\right)^{1/2}\left(-\frac{\partial U_G}{\partial x} - \frac{\partial V_G}{\partial y}\right) \tag{20}$$

We see that the vertical velocity at the top of the PBL is proportional to the curl of the surface stress and to the curl of the geostrophic wind. This qualitative result is in fact independent of how K is exactly specified. The vertical velocity can bee seen as a boundary condition for the inviscid flow above the boundary layer. The inflow of air in a cyclone due to friction at the surface causes an ascending motion at the top of the PBL and spins down the vortex by vortex compression (conservation of angular momentum). This mechanism is very important because it transfers the effect of boundary layer friction to the entire troposphere. Ekman pumping is illustrated in Fig. 5 .

2. SIMILARITY THEORY AND SURFACE FLUXES

Many physical processes in the atmosphere are too complicated to enable the derivation of parametrizations on the basis of first principles. Turbulence is such an example: although turbulent fluctuations are described by the equations of motion for a continuum fluid, it is very difficult to generate solutions of these equations and moreover the solutions show chaotic behaviour on very short time scales. Most of the time we are only interested in statistical averages. It is therefore common practice to rely on empirical relationships based on observations. Similarity theory provides the framework to organize and group the experimental data.

Similarity theory starts with the identification of the relevant physical parameters, then dimensionless groups are formed from the these parameters, and finally experimental data is used to find functional relations between dimensionless groups. When the functional relations are known, they can be used as part of a parametrization scheme. Because experimental data is always noisy and shows a lot of scatter it is important to limit as much as possible the number of dimensionless groups. It may for instance be difficult to find an empirical representation of noisy data when more than one or two independent parameters are involved. It is therefore advantageous to consider different parts of the boundary layer (surface layer, outer layer) and different limiting cases (neutral, very unstable etc.) separately, to simplify the problem and to limit the number of dimensionless groups that are relevant at the same time. The procedures are straightforward in principle (the Buckingham Pi dimensional analysis method; see e.g. Stull, 1988), but require experience and intuition in practice. The judgment of which parameters are important or unimportant is a crucial aspect of the analysis.

Similarity theory is used in virtually all PBL schemes that have been developed for atmospheric models. Different aspects of the boundary layer similarity are discussed in the following sections.

2.1 Surface-layer similarity

The surface layer is the shallow fraction of the PBL near the surface where the fluxes are approximately equal to the surface values. The surface layer is therefore often called the constant flux layer. Although the definition implies that z / h is much smaller than 1 in the surface layer, in practice the upper limit is often defined as the height where

$z / h = 0.1.$

The relevant parameters in the surface layer for the wind profiles are the momentum flux, the buoyancy flux and height above the surface

$$\frac{1}{\rho}|\tau_0| = \{(\overline{u'w'})_0^2 + (\overline{v'w'})_0^2\}^{1/2}, \tag{21}$$

$$-\frac{g}{\rho}(\overline{w'\rho'})_0 = \frac{g}{\theta_v}(\overline{w'\theta'_v})_0, \tag{22}$$

z (turbulence length scale).

The height above the surface is the length scale for turbulence because the size of the transporting eddies is confined by their distance from the surface. If the potential temperature and specific humidity are considered, we also need the kinematic fluxes of heat and moisture: $(\overline{w'\theta'})_0$ and $(\overline{w'q'})_0$. The following scales are defined:

$$u_* = \left|\frac{\tau_0}{\rho}\right|^{1/2} \quad \text{(friction velocity)} \tag{23}$$

$$L = \frac{-u_*^3}{k\frac{g}{\theta_v}(\overline{w'\theta_v'})_0} \quad \text{(Obukhov length)} \tag{24}$$

$$\theta_* = \frac{-(\overline{w'\theta'})_0}{u_*} \quad \text{(turbulent temperature scale)} \tag{25}$$

$$q_* = \frac{-(\overline{w'q'})_0}{u_*} \quad \text{(turbulent humidity scale)} \tag{26}$$

Since the non-neutral surface layer has two relevant length scales (z and L) all dimensionless quantities are written as function of z/L. Examples of dimensionless gradients and turbulence intensities are:

$$\frac{kzu_*}{(-\overline{u'w'})_0}\frac{\partial U}{\partial z} = \phi_M\left(\frac{z}{L}\right) \tag{27}$$

$$\frac{kzu_*}{(-\overline{v'w'})_0}\frac{\partial V}{\partial z} = \phi_M\left(\frac{z}{L}\right) \tag{28}$$

$$\frac{kz}{\theta_*}\frac{\partial \theta}{\partial z} = \phi_H\left(\frac{z}{L}\right) \tag{29}$$

$$\frac{kz}{q_*}\frac{\partial q}{\partial z} = \phi_Q\left(\frac{z}{L}\right) \tag{30}$$

$$\frac{\sigma_w}{u_*} = f_u\left(\frac{z}{L}\right) \tag{31}$$

$$\frac{\sigma_\theta}{\theta_*} = f_\theta\left(\frac{z}{L}\right) \tag{32}$$

note that

$$\frac{K_M}{kzu_*} = \frac{1}{\phi_M} \tag{33}$$

where $K_M = \dfrac{\tau_x}{dU/dz} = \dfrac{\tau_y}{dV/dz}$.

The dimensionless gradient functions (27)–(30) have been studied extensively with help of field experiments over homogeneous terrain. Fig. 6 illustrates this for ϕ_M with data from the Kansas experiment. Many empirical forms have been proposed for the dimensionless functions. The expressions for the unstable surface layer (often referred to as the Dyer and Hicks profiles; see Paulson 1970, Dyer 1974 and Hogstrom 1988 for a review) are:

$$\phi_M = \left(1 - 16\frac{z}{L}\right)^{-\frac{1}{4}} \tag{34}$$

$$\phi_{H, Q} = \left(1 - 16\frac{z}{L}\right)^{-\frac{1}{2}} \quad \text{for} \quad \frac{z}{L} < 0 \tag{35}$$

$$k = 0.4 \tag{36}$$

$$\tag{37}$$

and the linear relationship

$$\phi_M = \phi_{H, Q} = 1 + 5\frac{z}{L} \quad \text{for} \quad \frac{z}{L} > 0 \tag{38}$$

as originally proposed by Webb (1970) is fairly consistent with most data for $0 < z/L < 0.5$ (cf. Hogstrom, 1988). Analysis by Hicks (1976) of stable wind profiles above the flat homogeneous terrain of the "Wangara" site and by Holtslag and DeBruin (1988) of Cabauw data up to $z/L \approx 10$ resulted in the following expression (see also Beljaars and Holtslag, 1991)

$$\phi_M = 1 + a\frac{z}{L} + b\left(1 + c + d\frac{z}{L}\right)\exp\left(-d\frac{z}{L}\right) \tag{39}$$

$$\phi_H = 1 + \left(1 + \frac{2}{3}a\frac{z}{L}\right)^{\frac{3}{2}} + b\left(1 + c + d\frac{z}{L}\right)\exp\left(-d\frac{z}{L}\right) \tag{40}$$

where $a = 1, b = 0.667, c = 5$ and $d = 0.35$. This expression behaves like (38) for small z/L values and approaches $\phi_M \sim a\,z/L$ for large z/L. The 3/2 power in ϕ_H has been introduced to make ϕ_H/ϕ_M proportional to $(z/L)^{1/2}$ for large values of z/L (see discussion on stability functions in section 3.3).
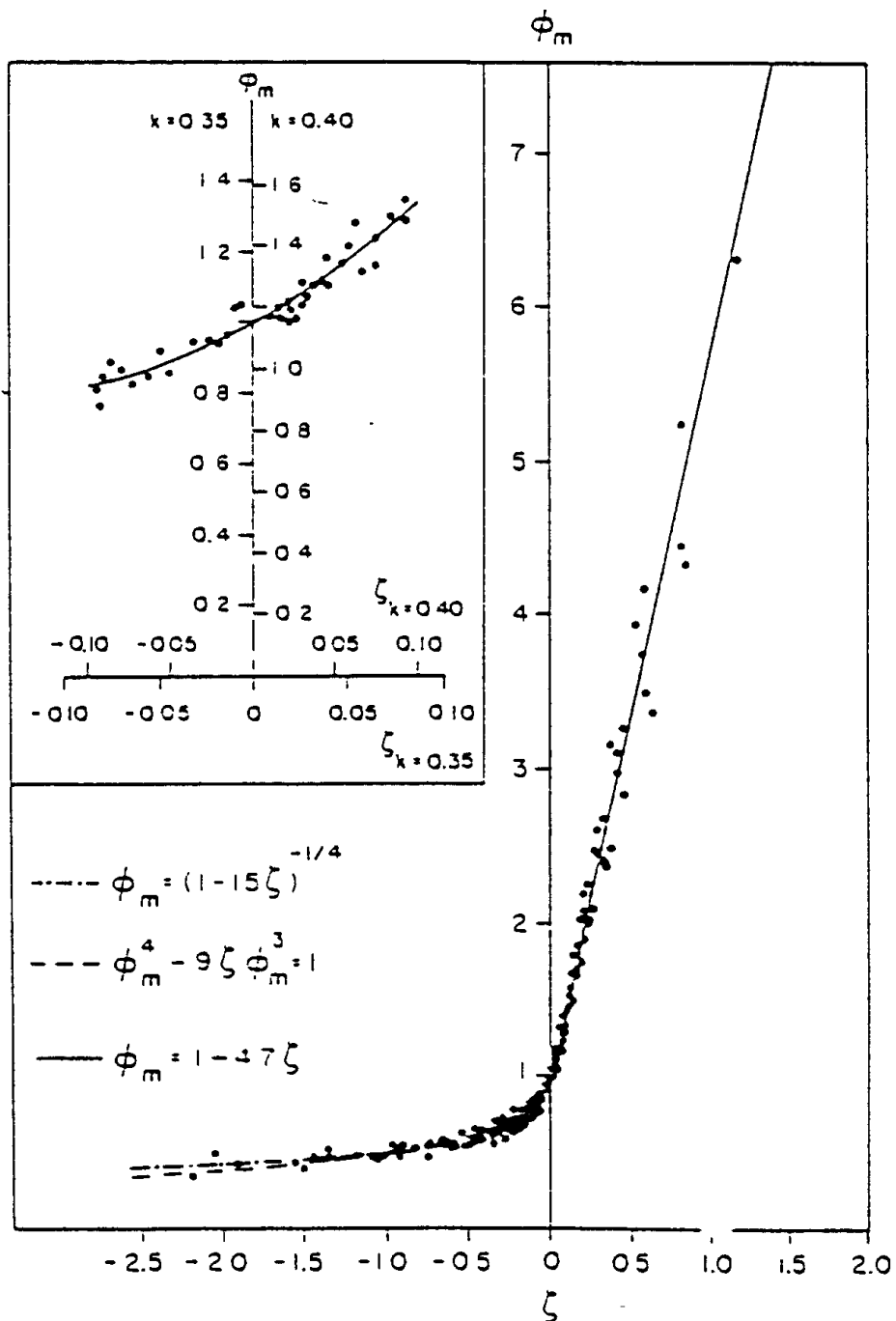
Figure 6. Comparison of dimensionless wind shear observations with interpolation formulas (after Businger et al. 1971; $\zeta = z/L$).
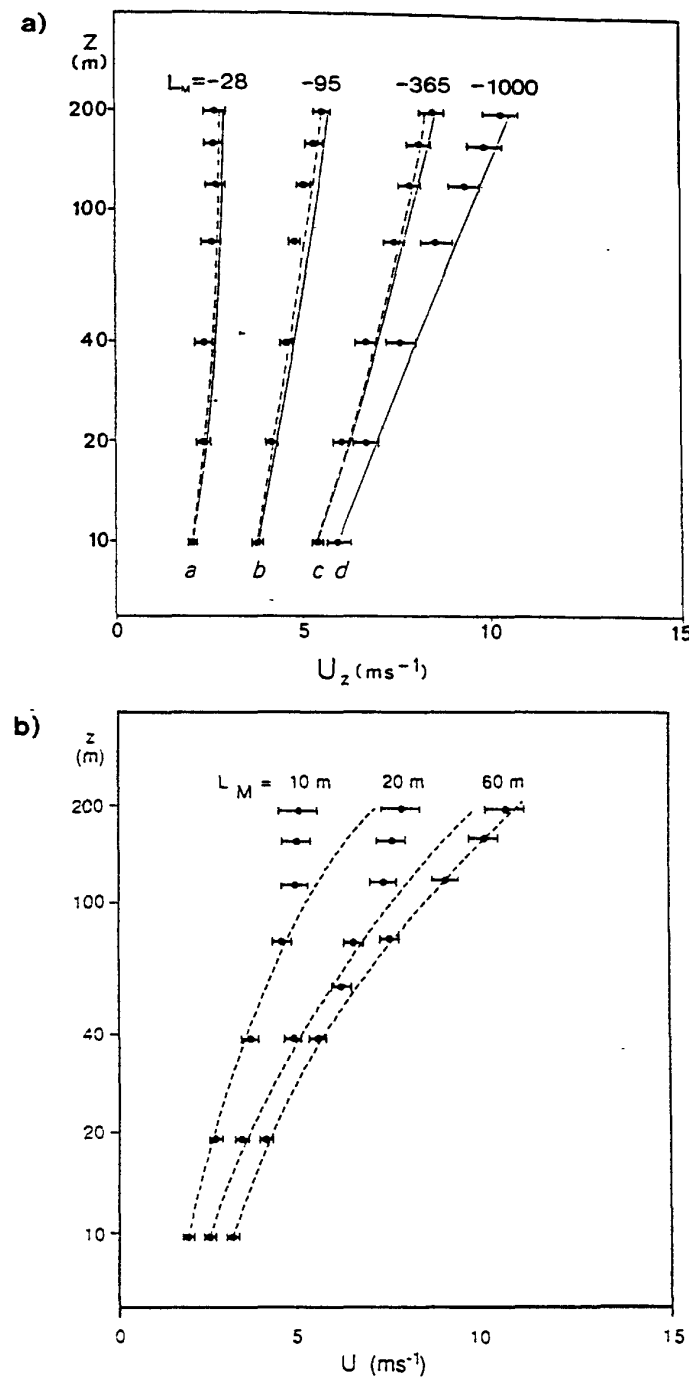
Figure 7. Wind profiles extrapolated from observed 10 m wind according to (2.1.21-22) with (2.1.25) and (2.1.28) in comparison with observations up to 200 m (Cabauw). The upper and lower panel represents unstable and stable stratification respectively. Lm indicates the stability class as an average over a number of observations. The dots and error bars represent averages and standard deviations of observations (from Holtslag 1984).

The gradient functions can be integrated to profiles for wind, potential temperature and specific humidity

$$U = \frac{\tau_x}{\rho k u_*}\left[\ln\left(\frac{z}{z_{0\mathrm{M}}}\right) - \Psi_{\mathrm{M}}\left(\frac{z}{L}\right)\right] \tag{41}$$

$$V = \frac{\tau_y}{\rho k u_*}\left[\ln\left(\frac{z}{z_{0\mathrm{M}}}\right) - \Psi_{\mathrm{M}}\left(\frac{z}{L}\right)\right] \tag{42}$$

$$\theta - \theta_s = \frac{(-\overline{w'\theta'})_0}{k u_*}\left[\ln\left(\frac{z}{z_{0\mathrm{H}}}\right) - \Psi_{\mathrm{M}}\left(\frac{z}{L}\right)\right] \tag{43}$$

$$q - q_s = \frac{(-\overline{w'q'})_0}{k u_*}\left[\ln\left(\frac{z}{z_{0\mathrm{Q}}}\right) - \Psi_{\mathrm{M}}\left(\frac{z}{L}\right)\right] \tag{44}$$

with

$$\Psi_{\mathrm{M}} = 2\ln\{(1+x)/2\} + \ln\{(1+x^2)/2\} - \mathrm{atan}(x) + \pi/2 \tag{45}$$

$$\Psi_{\mathrm{H,Q}} = 2\ln\{(1+x^2)/2\} \quad \text{for} \quad \frac{z}{L} < 0 \tag{46}$$

where

$$x = \left(1 - 16\frac{z}{L}\right)^{\frac{1}{4}} \tag{47}$$

and

$$\Psi_{\mathrm{M}} = -a\frac{z}{L} - b\left(\frac{z}{L} - \frac{c}{d}\right)\exp\left(-d\frac{z}{L}\right) - \frac{bc}{d} \tag{48}$$

$$\Psi_{\mathrm{H}} = 1 - \left(1 + \frac{2}{3}a\frac{z}{L}\right)^{\frac{3}{2}} - b\left(\frac{z}{L} - \frac{c}{d}\right)\exp\left(-d\frac{z}{L}\right) - \frac{bc}{d} \quad \text{for} \quad \frac{z}{L} > 0 \tag{49}$$

This can be derived from the gradient functions with help of the relationship $\phi = 1 - (\eta)\, \mathrm{d}\Psi/\mathrm{d}\eta$, where $\eta = z/L$. Examples of wind profiles according to the empirical forms of (45) and (48) are shown in Fig. 7 in comparison with data.

It is clear that these functions play a crucial role in parametrization schemes. The gradient functions provide direct expressions for exchange coefficients as they relate fluxes to gradients. The integral profile functions are generally used in models that have a model level in the surface layer to specify the profiles between the lowest model level and the surface. The expressions (41) to (44) can in fact be seen as finite difference forms for the layer between the surface and the lowest model level.

Limiting cases in surface layer similarity

In determining analytical forms for the similarity functions it is often useful to consider their asymptotic behaviour. The neutral limit ($z/L = 0$) and the free convection limit ($-z/L \gg 1$) are of particular interest because they provide information to limit the degrees of freedom in choosing analytical expressions.

In the neutral limit with $z/L = 0$, the Obukhov length drops out as a relevant scale and therefore the dimensionless

wind gradient has to be constant. The dimensional wind gradient ϕ_M is by definition equal to 1 because the empirical constant is absorbed in the definition and is called the Von Karman constant. The exact value of the Von Karman constant has been subject of considerable debate. Values between 0.35 and 0.42 have been proposed, but 0.4 is the most widely accepted value now (e.g. Hogstrom, 1988).

The other limiting case with $-z/L \gg 1$ is called the free convection limit. A large value for $-z/L$ implies that the production of turbulence by buoyancy is much larger than the production by wind shear and that the friction velocity u_* is irrelevant as scaling quantity. The only way to obtain independence of u_* in the dimensionless potential temperature gradient expression is by choosing a 1/3 power law for $-z/L \gg 1$, as L is proportional to u_*^3, by definition:

$$\frac{kzu_*}{(\overline{w'\theta'})_0}\frac{\partial\theta}{\partial z} = \phi_H\left(\frac{z}{L}\right) \sim \left(-\frac{z}{L}\right)^{\frac{1}{3}} \tag{50}$$

Alternatively a convective velocity scale can be defined based on the on the buoyancy flux

$$w_{*s} = \left[\frac{g}{\theta_v}(\overline{w'\theta'}_v)_0 z\right]^{\frac{1}{3}} \tag{51}$$

resulting in

$$\frac{kzw_{*s}}{(\overline{w'\theta'})_0}\frac{\partial\theta}{\partial z} = \text{constant} \tag{52}$$

The free convection velocity represents physically the velocity that large eddies (e.g. thermals) typically have in the convective boundary layer. It should be noted that equation (35) does not satisfy the constraint as imposed by the free convection limit. In practice however (35) fits data as accurately as expressions that tend to $(-z/L)^{-1/3}$ for large $-z/L$.

Another example of the free convection limit is the scaling relation for the variances of velocity and temperature fluctuations (see also Fig. 8):

$$\frac{(\overline{w'^2})^{\frac{1}{2}}}{u_*} = c_w\left(-\frac{z}{L}\right)^{\frac{1}{3}} \tag{53}$$

$$\frac{(\overline{\theta'^2})^{\frac{1}{2}}}{\theta_*} = c_\theta\left(-\frac{z}{L}\right)^{-\frac{1}{3}} \tag{54}$$

With the definitions of L and θ_* it can be verified that u_* drops out of these relations. Alternatively the same forms can be expressed in terms of the free convection velocity without using u_*. The advantage of the expression in z/L is that it provides a limiting form for large z/L. These examples clearly illustrate the strength of similarity theory. For the neutral and free convection limit the similarity arguments even provide the shape of the functions, experiments are only needed to determine the value of the constants (e.g. the Von Karman constant).
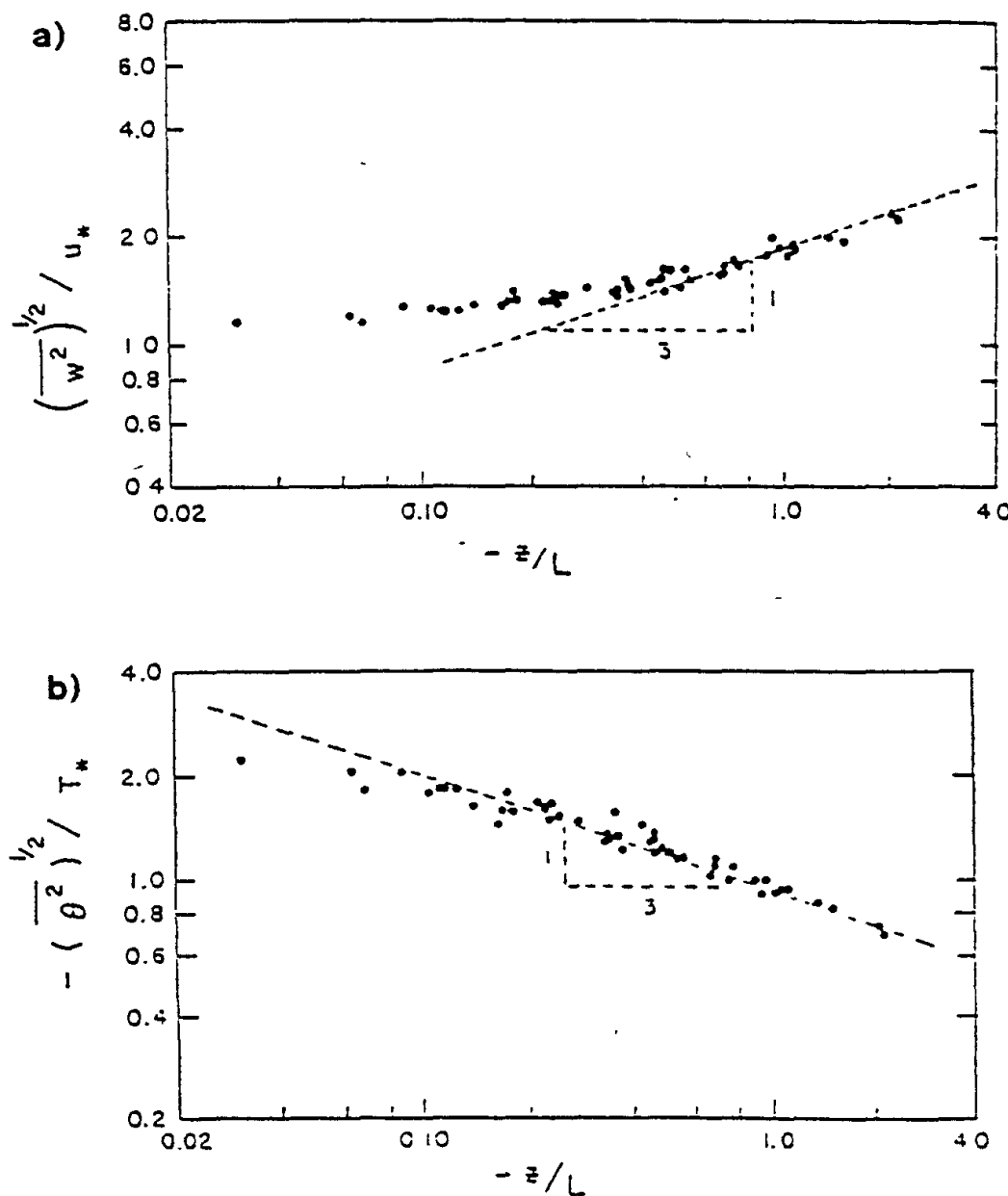
Figure 8. Examples of free convection scaling for large $-z/L$. Standard deviations of vertical velocity and temperature fluctuations.

2.2 The outer layer

The outer layer of the PBL is the remaining part of the boundary layer above the surface layer. The fluxes are not constant as in the surface layer but decrease monotonically from their surface values to small values at the top of the PBL (see Fig. 9 for the convective boundary layer). The surface layer parameters are also relevant in the outer layer. Additionally, the boundary layer height h (length scale) and in the extratropics the Coriolis parameter f (inverse time scale) enter the problem.

Neutral PBL

If the boundary layer height is not determined externally (e.g. by a capping inversion) but by the boundary layer processes themselves then the boundary layer height must be proportional to the only length scale in the problem namely u_*/f. The relevant parameters are: u_*, f, and z; the velocity profiles are usually written as differences with the geostrophic wind as so-called velocity defect laws:

$$\frac{U - U_{\mathrm{G}}}{u_*} = f_u\left(\frac{z\,u_*}{f}\right)$$

(55)

$$\frac{V - V_{\mathrm{G}}}{u_*} = f_v\left(\frac{z\,u_*}{f}\right)$$

(56)
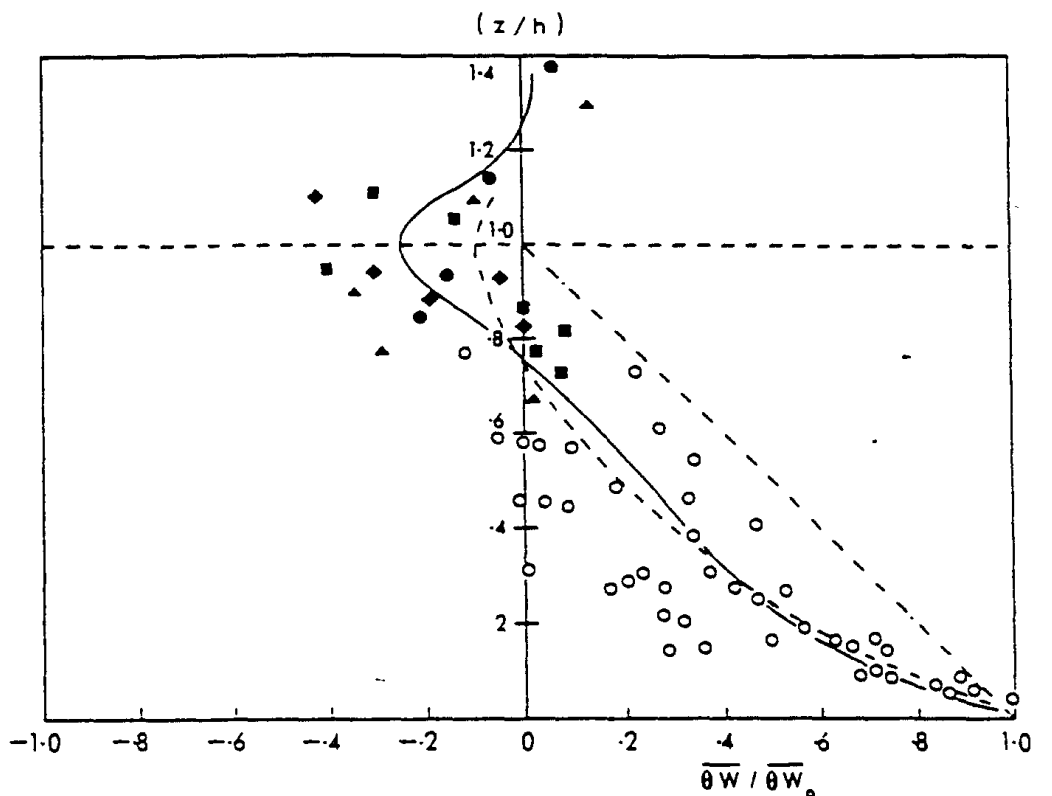
Figure 9. Height dependence of the kinematic heat flux in the convective boundary layer. The solid line refers to a model with entrainment; the dashed line refers to a model without entrainment.
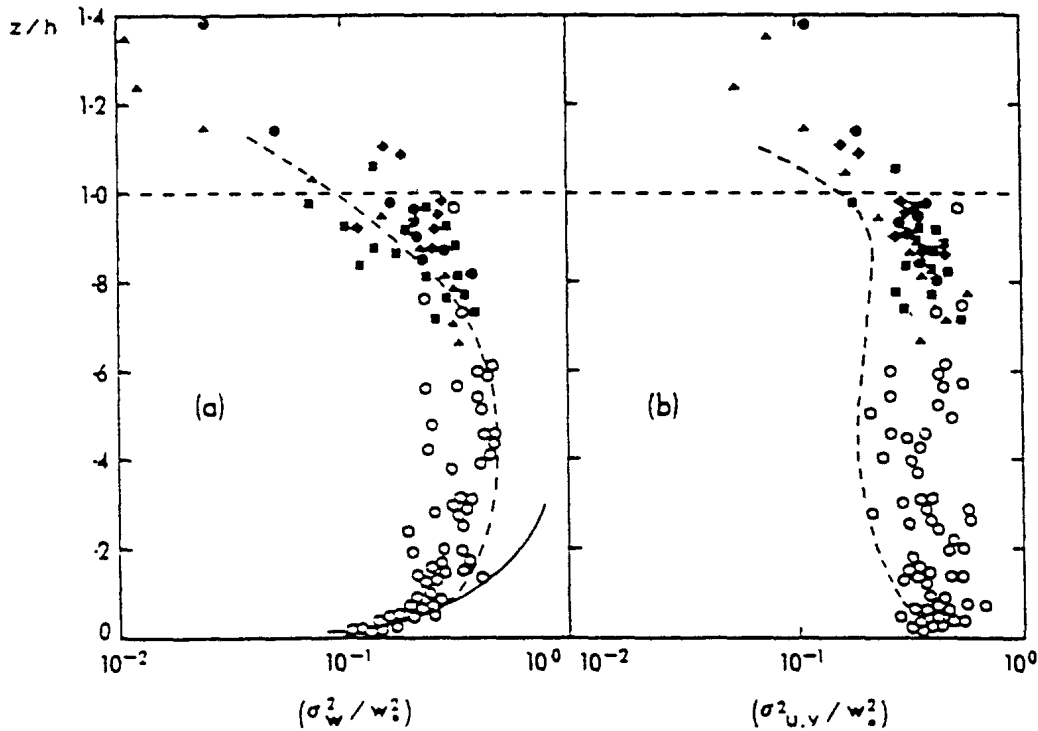
Figure 10. Example of mixed layer scaling for the horizontal and vertical turbulent velocity fluctuations.

Convective boundary layer (mixed layer scaling)

In the convective boundary layer the PBL height is determined by a capping inversion at height h which can be interpreted as an independent parameter. Formally also the friction velocity u_* and the Coriolis parameter f play a role. They are often omitted because the wind turning is small in the well mixed layer and $-z/L$ (which is by definition larger than $-0.1\,h/L$) is often large. The remaining relevant parameters are $(\overline{w'\theta'_v})_0$, h, and z, from which we define:

$$\text{velocity scale} \quad w_* = \left[\frac{g}{\theta_v}(\overline{w'\theta'_v})_0 h\right]^{\frac{1}{3}} \tag{57}$$

$$\text{temperature scale} \quad \theta_* = -\frac{(\overline{w'\theta'})_0}{w_*} \tag{58}$$

The dimensionless gradients of wind temperature and specific humidity are not very interesting in this case because the gradients are very small. The turbulent exchange is so strong in the convective boundary layer that the profiles are nearly uniform (well mixed). Mixed layer scaling, however, applies to velocity and temperature fluctuations e.g. σ_u/w_*, σ_v/w_*, σ_w/w_* and σ_θ/θ_* are functions of z/h (see Fig. 10 for $\sigma_{u,v,w}$).

Stable boundary layer (local scaling)

The same principles as used for the convective boundary layer could be applied to the stable boundary layer. However, the friction velocity can not be omitted as friction is the only source of turbulence production.

To limit the number of independent parameters Nieuwstadt (1984) introduced the idea of local scaling which can be made plausible in the following way. In the stable boundary layer turbulence is generated by shear production and destroyed by buoyancy and viscous dissipation. Since buoyancy is acting in the vertical component it tends to limit the vertical extent over which the mixing takes place and therefore limits the turbulence length scale. The decoupling of turbulence from the surface suggest that the local fluxes might be more suitable as direct scaling parameters. The strength of this idea lies in the fact that the resulting functions are necessarily the same as the ones for the surface layer since the local fluxes are equal to the surface fluxes when the surface is approached. This means that experimental data from the surface layer and the outer layer can be combined. For models with local closure (as in the ECMWF model) it also means that the closure scheme for the surface layer and the outer layer can be the same.

In the framework of local scaling the relevant parameters are: the local fluxes τ/ρ and $\overline{w'\theta'_v}$,the buoyancy parameter g/θ_v and height z. From these we define:

$$\Lambda = \frac{-|\tau/\rho|^{3/2}}{k\frac{g}{\theta_v}\overline{w'\theta'_v}} \quad \text{(local Obukhov length) .} \tag{59}$$

Local scaling implies that dimensionless quantities are functions of z/Λ instead of z/L. Examples of local scaling are given in Fig. 12 ; the height dependence of momentum and heat fluxes is illustrated in Fig. 11 .

For large z/Λ the turbulence length scale is Λ and the presence of the surface should have no influence. This implies that z should drop out of the scaling relations. The consequence for the dimensionless gradient functions is that they become linear in z/Λ for large z/Λ because they have z as a length scale in their definition. The principle that dimensionless functions become independent of z is called z-less scaling. The consequence in Fig. 12 is that the empirical functions tend to a constant for large z/Λ.

The different scaling regimes of the boundary layer are summarized in Fig. 13 for the unstable and stable PBL. The dimensionless height z/h and the dimensionless stability parameter h/L are used to delineate the different scaling regimes.

2.3 Matching of surface and outer layer (drag laws)

The profile functions for the neutral outer layer written in velocity defect form must be logarithmic for $z/h \to 0$ and must match the surface layer profiles. With the coordinate system aligned with the surface wind $(\overline{v'w'})_0 = 0$ and neutral stability:

surface layer limit for $z/z_{0M} \to \infty$:

$$\frac{U}{u_*} = \frac{1}{k}\ln\left(\frac{z}{z_{0M}}\right) \tag{60}$$

outer layer limit for $z/h \to 0$:

$$\frac{U - U_G}{u_*} = \frac{1}{k}\ln\left(\frac{zf}{u_*}\right) + \text{const} \tag{61}$$

$$V = 0 \tag{62}$$
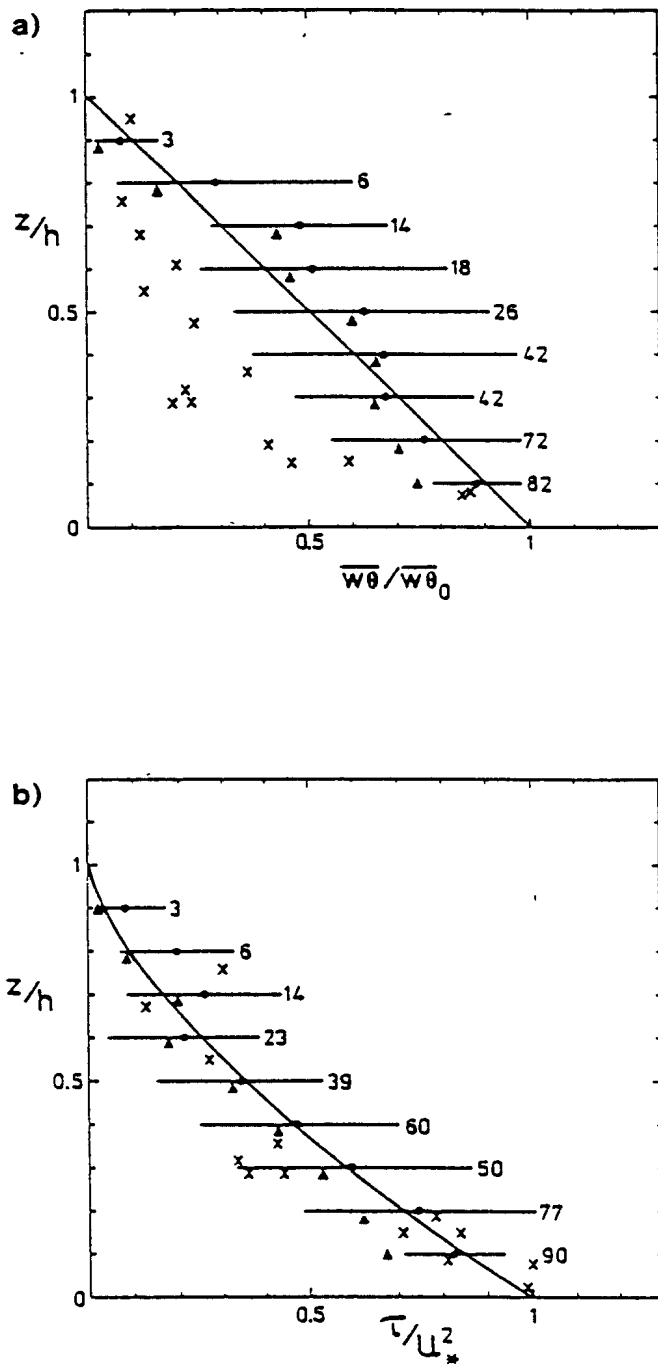
Figure 11. Height dependence of the kinematic heat flux and the kinematic momentum flux in the stable boundary layer (from Nieuwstadt 1984)

Matching the surface and outer layer forms leads to (Tennekes, 1973):

$$\frac{U_G}{u_*} = \frac{1}{k}\ln\left(\frac{u_*}{f z_{0M}}\right) - \frac{A}{k} \tag{63}$$

$$\frac{V_G}{u_*} = -\frac{B}{k}$$

(64)

The constants A and B can be measured and express in dimensionless form the drag and the ageostrophic angle of the surface wind with respect to the geostrophic forcing. Such "drag-laws" can be applied directly to models that do not resolve the PBL, but are also an important diagnostic tool. In models that do resolve the boundary layer, the drag law can be computed (e.g. in one column tests) and compared with data for the steady state PBL (see Fig. 14).

For non-neutral flow it is often assumed that A and B are functions of the stability parameter $\mu = u_*/(fL)$. Such an assumption is quite arbitrary but works fairly well in practice.
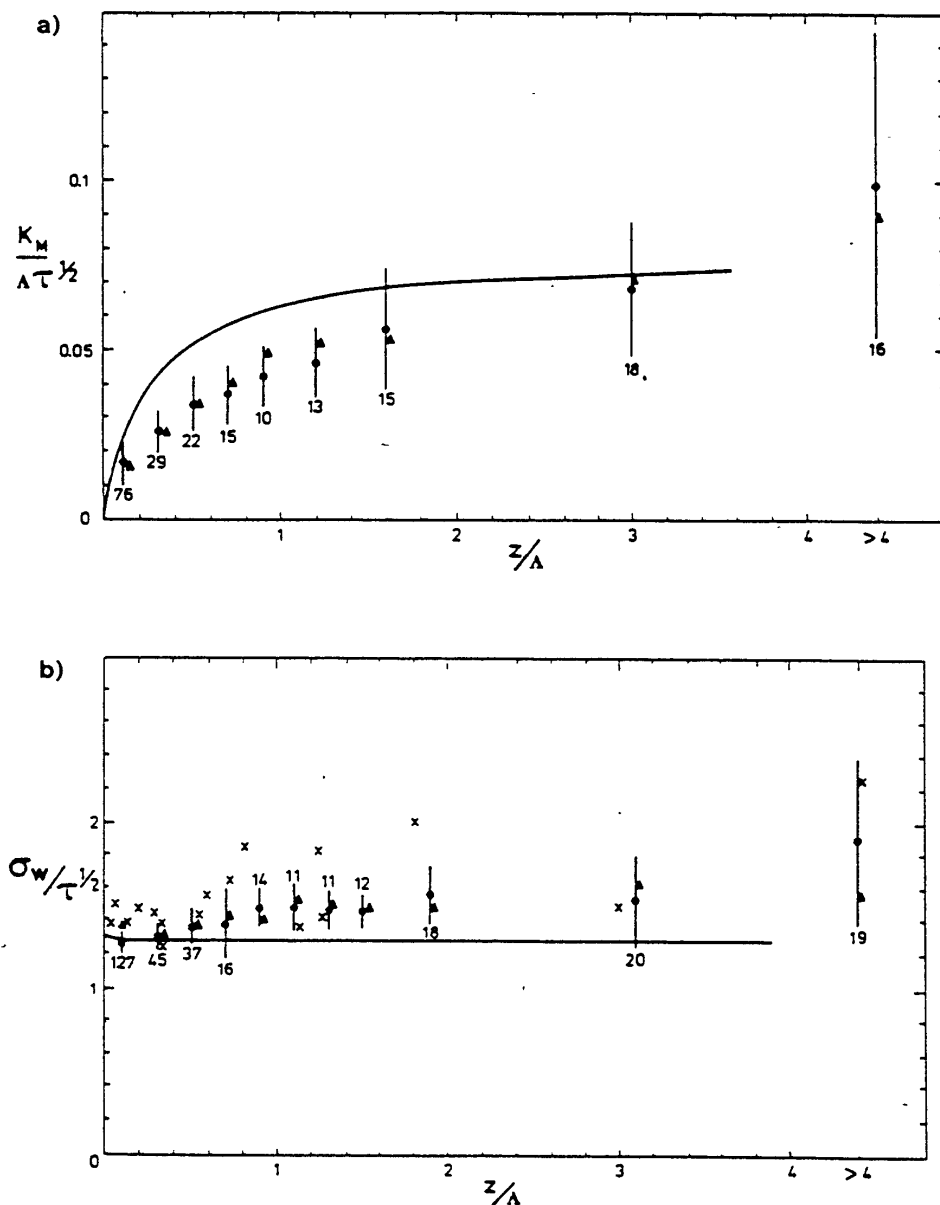
Figure 12. Two examples of local scaling (a) exchange coefficient for momentum and (b) the standard deviation of vertical velocity in the stable boundary layer (from Nieuwstadt 1984).
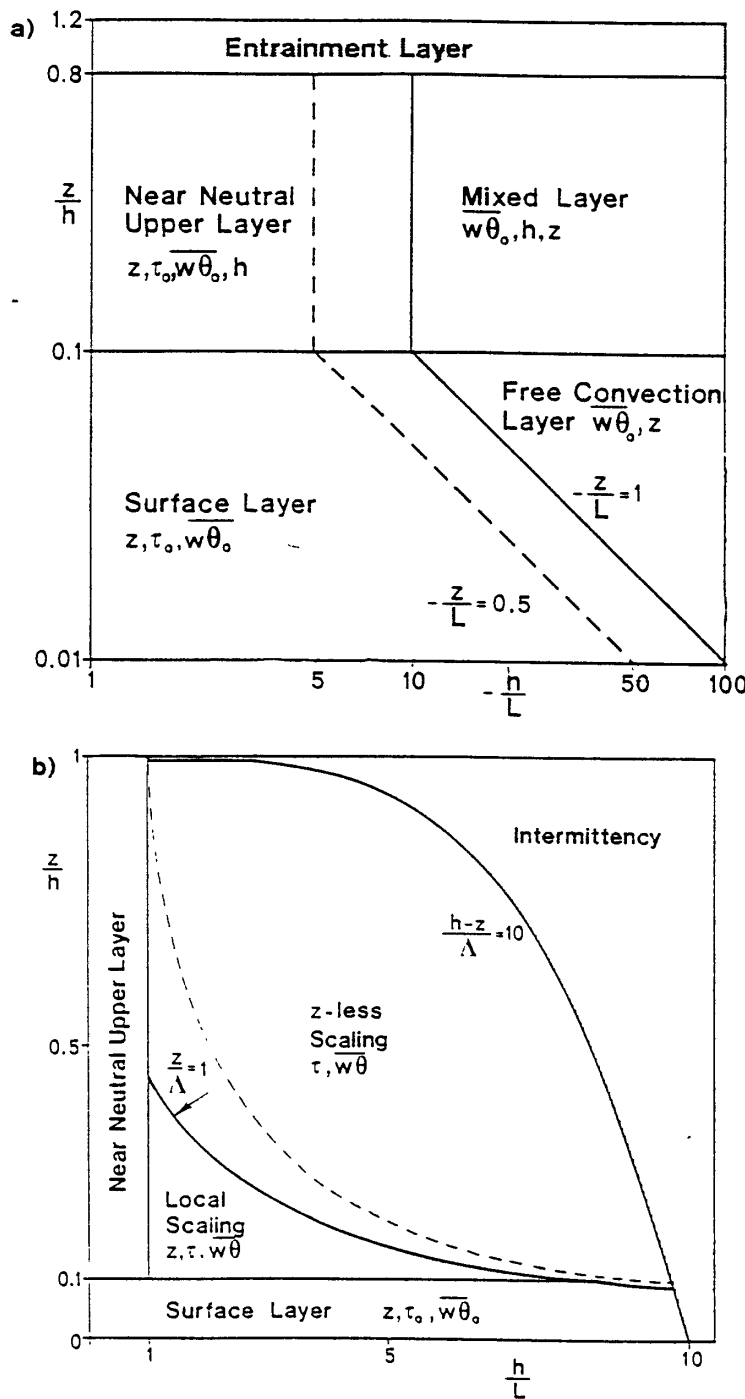
Figure 13. Scaling regions in the unstable (upper panel) and the stable (lower panel) PBL (from Holtslag and Nieuwstadt 1986).
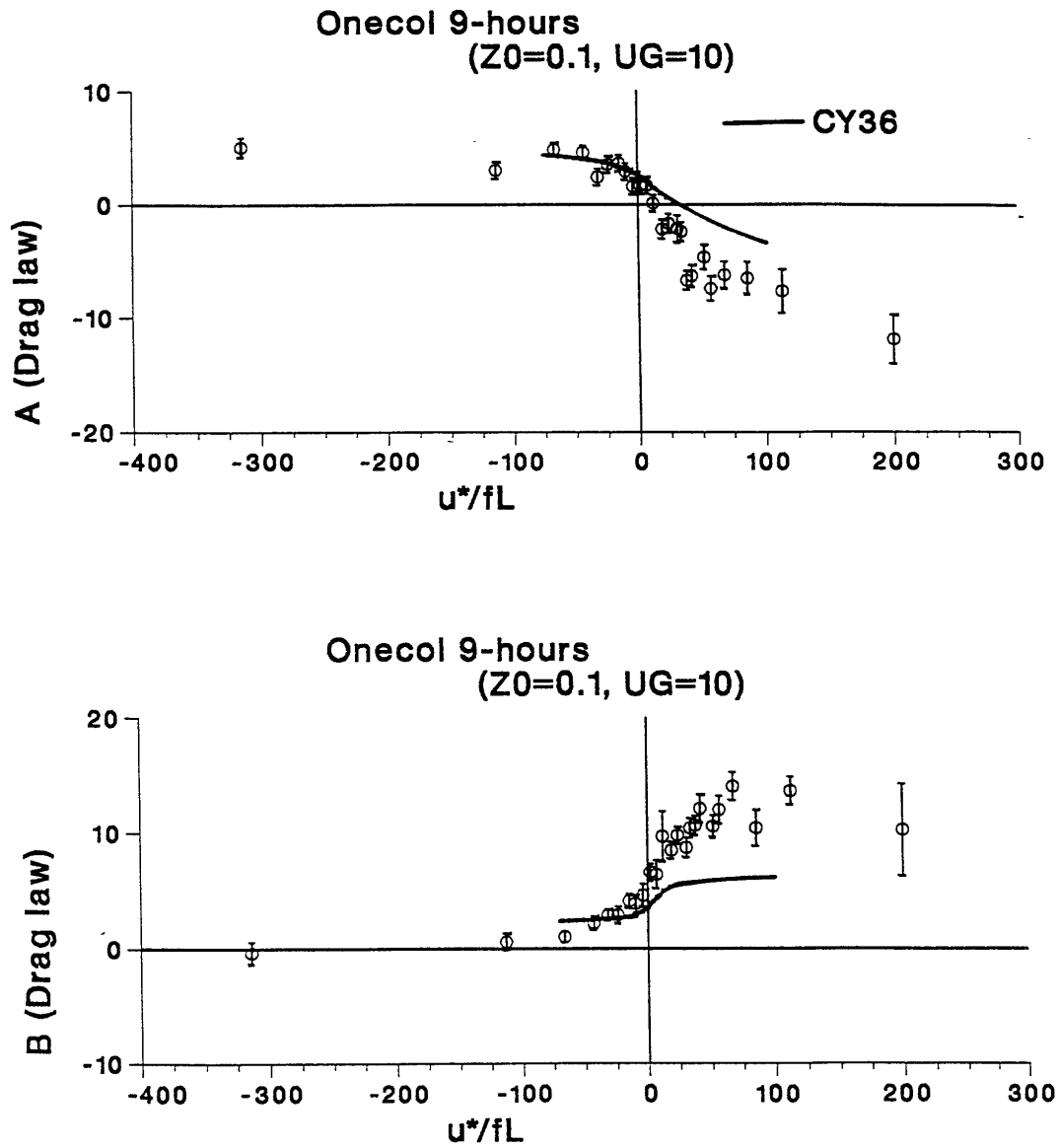
Figure 14. Constants A and B in the geostrophic drag law according to Wangara data (Clarke and Hess 1974) in comparison with the ECMWF (CY34) model formulation after 9 hours of integration (as a function of stability parameter fu_*/L).

2.4 Surface boundary conditions and surface fluxes

The parametrization of the PBL introduces at the same time the need for boundary conditions at the surface. The boundary conditions are simply vanishing velocity and specified temperatures and specific humidities at the surface. Over sea the temperature is specified and the specific humidity is the saturation value at the sea surface temperature. Specification of temperature and specific humidity over land is part of the land surface parametrization scheme. In some models, however, the surface energy balance equation is used over land to eliminate the surface temperature and surface specific humidity. This is often referred to as the Penman Monteith concept (see Monteith 1981), which is not discussed here.

Looking more carefully at the boundary conditions, one realizes that an additional parametrization problem arises. The boundary conditions are connected to the surface roughness lengths which are extremely important to the surface fluxes. To illustrate this we assume that we have a model level near the surface in the constant flux layer at a specified height z_1 (in the ECMWF model ≈ 32 m). The surface layer profiles are used to specify the boundary condition:

$$U = \frac{\tau_{x0}}{\rho k u_*}\left[\ln\left(\frac{z_1}{z_{0M}}+1\right)-\Psi_M\left(\frac{z_1}{L}\right)\right] \tag{65}$$

$$V = \frac{\tau_{y0}}{\rho k u_*}\left[\ln\left(\frac{z_1}{z_{0M}}+1\right)-\Psi_M\left(\frac{z_1}{L}\right)\right] \tag{66}$$

$$\theta - \theta_s = \frac{(-\overline{w'\theta'})_0}{k u_*}\left[\ln\left(\frac{z_1}{z_{0H}}+1\right)-\Psi_M\left(\frac{z_1}{L}\right)\right] \tag{67}$$

$$q - q_s = \frac{(-\overline{w'q'})_0}{k u_*}\left[\ln\left(\frac{z_1}{z_{0Q}}+1\right)-\Psi_M\left(\frac{z_1}{L}\right)\right] \tag{68}$$

The logarithmic profiles are written in a way that U, V, θ and q have their surface values for $z = 0$ (a displacement height equal to the roughness length has been added to the vertical coordinate). The integration constants in the logarithmic profiles are called roughness lengths because they are related to the small scale surface inhomogeneities that determine the surface drag. In general the viscous forces play no role at all in the surface drag (except over a very smooth sea); the pressure forces on the roughness elements transfer the wind stress to the surface (form drag) and do so more efficiently than viscous forces because the height of roughness elements tends to be larger than the thickness of the viscous layer. For heat and moisture the situation is slightly different. Form drag has no equivalent for scalar quantities. The air-surface transfer is through an inter-facial sub-layer where molecular transfer domnates. This implies that the roughness lengths for momentum, heat and moisture are generally different.

TABLE 2. TYPICAL ROUGHNESS LENGTHS Z_* (Wieringa 1986)

| Ground cover	Roughness length (m)
Water or ice (smooth) (over water z_{0M} increases with wind speed	10^{-4}
Mown grass	10^{-2}
Long grass, rocky ground	0,05
Pasture land	0.20
Suburban housing	0.6
Forest, cities	1–5
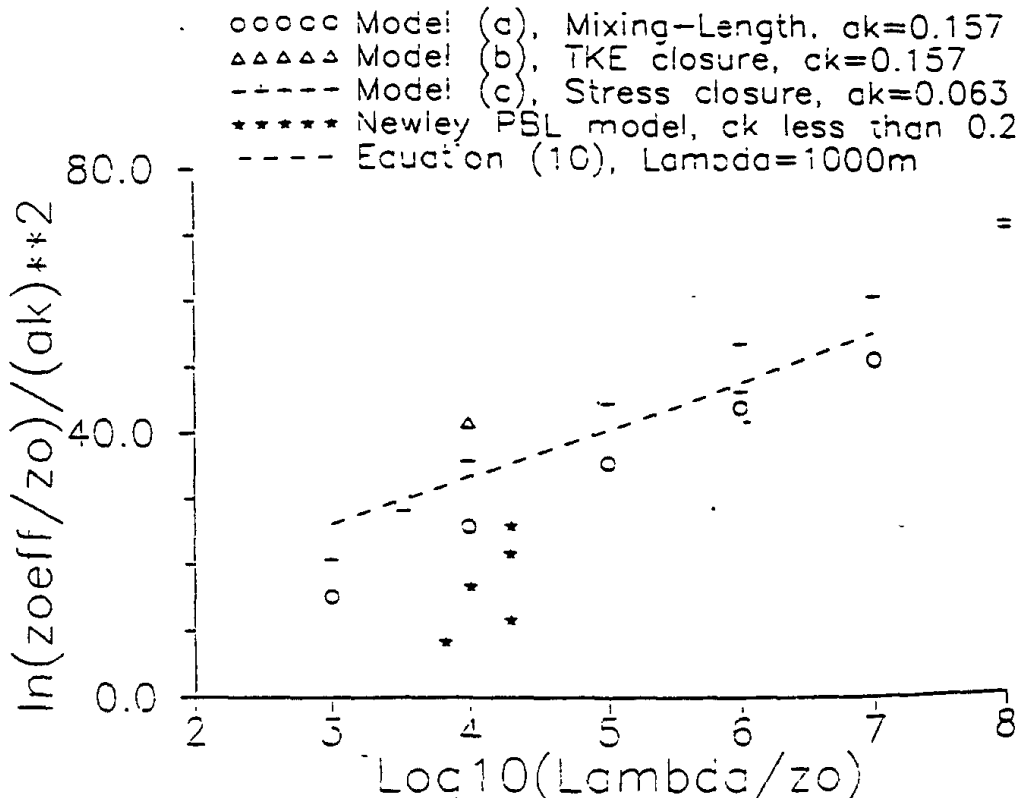
Figure 15. Variation of the effective roughness length z_{0M}^{eff} as a function of λ / z_{0M}, where λ is the wavelength of 2-dimensional sinusoidal orography with amplitude a. Different models are compared (Taylor et al. 1989).

It is important to realize that the specification of the surface roughness lengths is an important aspect of the parametrization since the they determine to a large extent the surface fluxes. The roughness length is a surface characteristic and is related to its geometry, but the only way to define it is by means of the logarithmic profile. Measuring the logarithmic profile well away from the surface is the only way of determining z_{0M} for a uniform terrain. For a large scale model with grid spacings of the order of 100 km many terrain inhomogeneities exist that affect the surface drag. The effects of sub-grid terrain effects and sub-grid orography are accounted for by defining and "effective roughness length", which is defined as the roughness length that gives the correct surface flux in the parametrization. The roughness lengths are often derived from land-use maps with an extra contribution from the variance of the sub-grid orography (see Table 2). A data base for land use is provide by Wilson and Henderson-Sellers (1985). A review of sub-grid averaging is provided by Mason (1988) and Taylor et al. (1989). The issue of sub-grid averaging of z_{0H} and z_{0Q} has only very recently received attention (see Wood and Mason 1991;Mason 1991; Beljaars and Holtslag, 1991).

Fig. 15 illustrates empirical data on the relation between the amplitude of not too steep sub-grid orography and the aerodynamic roughness length. Steep orography is more difficult to parametrize (see Mason, 1988 for a review). The difference between the roughness length for heat and momentum can be quite large as illustrated in Fig. 16 . Recent studies suggest that terrain inhomogeneities have a large impact on the ratio z_{0H} and z_{0M} (see Mason 1991).

Specification of the surface roughness lengths over sea is even more important than over land particularly for heat and moisture because with the fixed boundary conditions for temperature and moisture the sea is in principle an infinite source of energy to the model. Currently the ECMWF model has equal values for momentum heat and

moisture all specified with help of the Charnock relation

$$z_{0M} = \max\left(0.018\frac{u_*^2}{g}, 1.15 \times 10^{-5} \text{ m}\right) \tag{69}$$

$$z_{0H} = z_{0Q} = z_{0M} \tag{70}$$
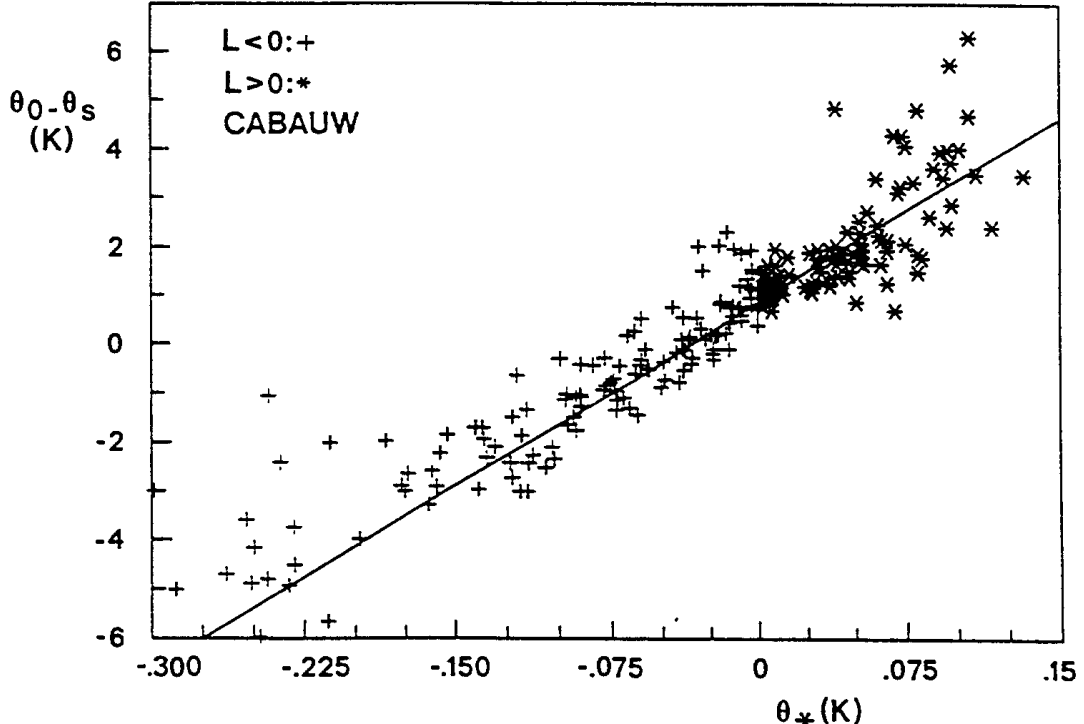
Figure 16. Temperature difference over the inter-facial sub-layer for short grass. By definition: $\theta_0 - \theta_s = (\theta_*/k)\ln(z_{0M}/z_{0H})$. This figure illustrates the possible difference between the roughness length for momentum and for heat particularly when an "effective value" is used. (Cabauw data; Beljaars and Holtslag, 1991).

This parametrization does not satisfy the smooth surface limit at low wind speed where viscous forces dominate (with scaling on ν/u_*). Furthermore Smith (1988) argues in a recent review that the increase of the roughness length with increasing wind speed does not apply to heat and moisture. An alternative which combines the smooth surface limit with the conclusions of Smith's review is:

$$z_{0M} = 0.018\frac{u_*^2}{g} + 0.11\frac{\nu}{u_*} \tag{71}$$

$$z_{0H} = 1.4 \times 10^{-5} + 0.40\frac{\nu}{u_*} \tag{72}$$

$$z_{0Q} = 1.3 \times 10^{-4} + 0.62\frac{\nu}{u_*} \tag{73}$$

The two formulations are compared with data by Large and Pond (1982) in the Figs. 17 – 19 .
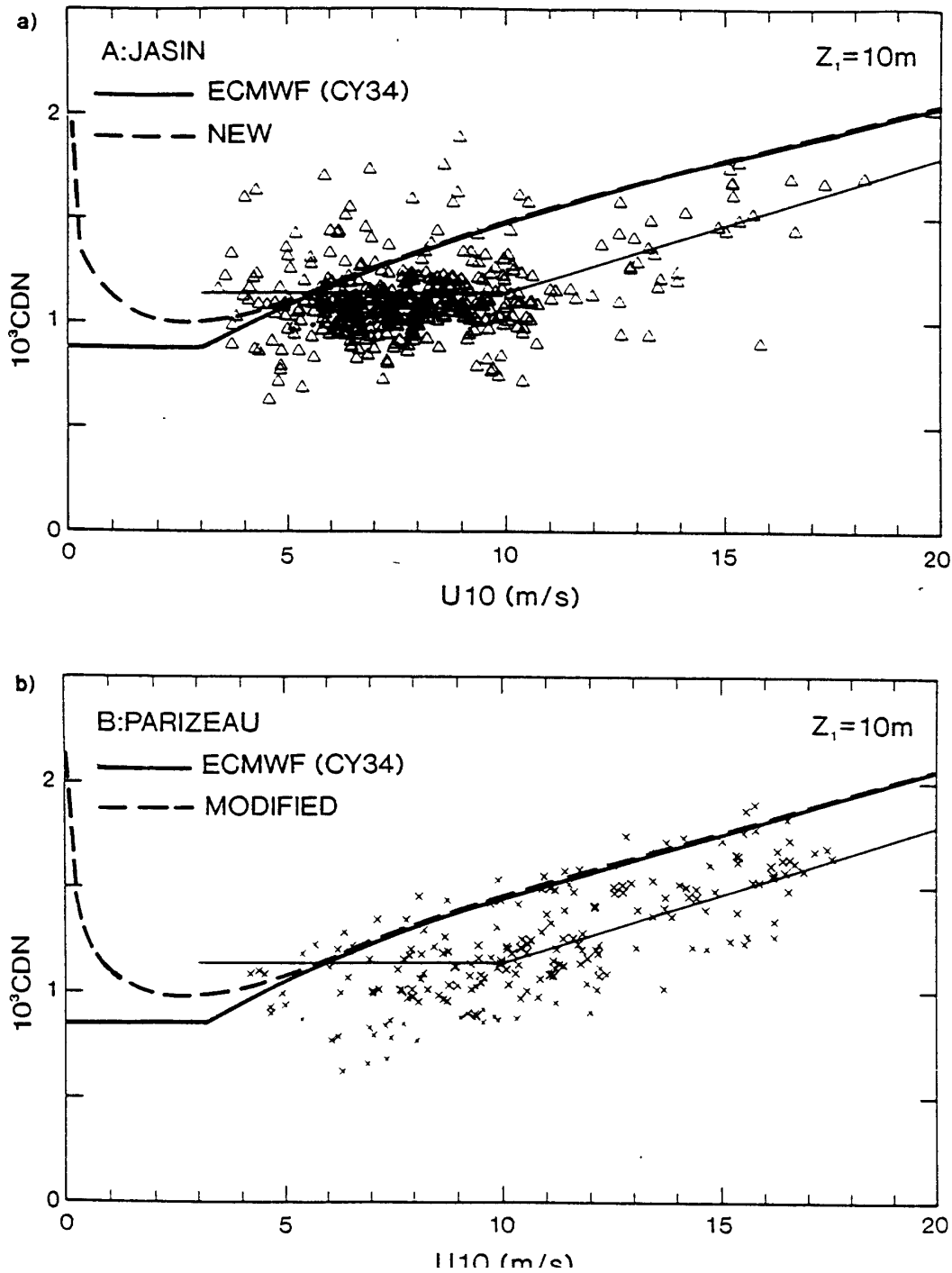
Figure 17. Neutral transfer coefficients for momentum between the sea surface and the 10 m level. The observations were published by Large and Pond (1982); the thick solid and dashed line represent Eqs. (69) and (71) respectively. C_{MN} is related to z_{0M} by means of: $C_{MN} = \{k / \ln(z_1 / z_{0M})\}^2$
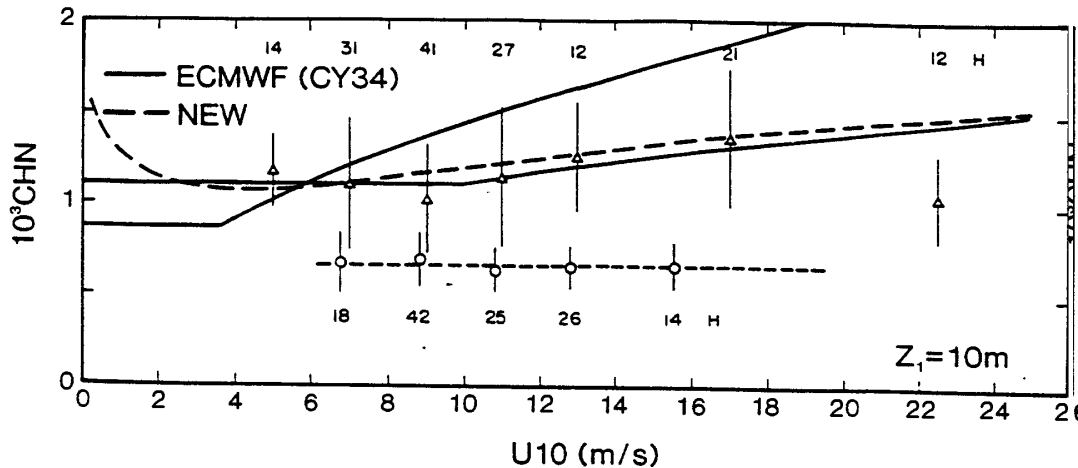
Figure 18. Neutral transfer coefficients for heat between the sea surface and the 10 m level. The observations were published by Large and Pond (1982); the thick solid and dashed line represent Eqs. (69) – (70) and (71) – (72), respectively. C_{HN} is related to z_{0M} and z_{0H} by means of: $C_{HN} = \{k/\ln(z_1/z_{0M})\}\{k/\ln(z_1/z_{0H})\}$, where z_1 is the 10 m level (normally the height of the lowest model level).
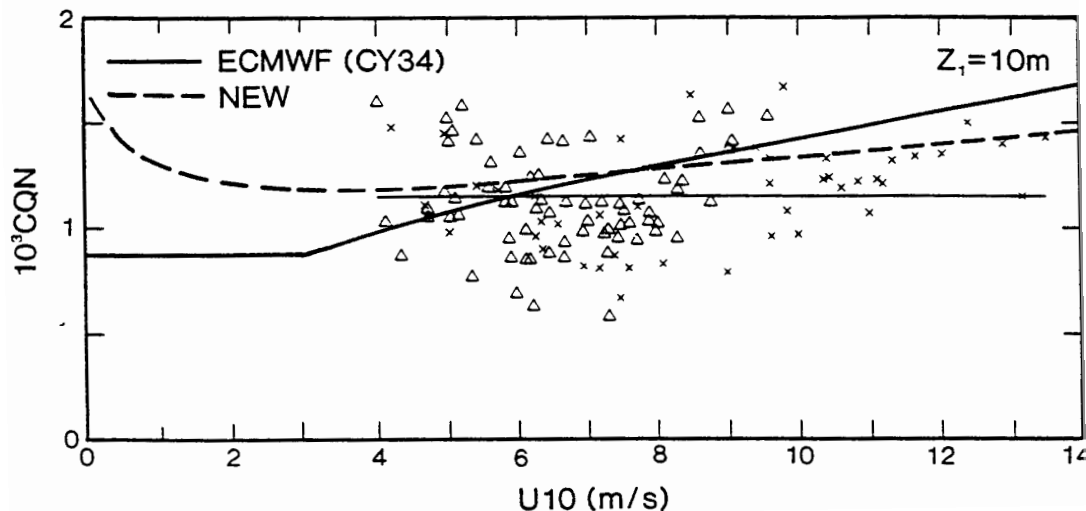
Figure 19. Eqs. (69), (70), (71) and (73), respectively. C_{QN} is related to z_{0M} and z_{0Q} by means of:
$C_{QN} = \{k/\ln(z_1/z_{0M})\}\{k/\ln(z_1/z_{0Q})\}$, where z_1 is the 10 m level (normally the height of the lowest model level.

3. PBL SCHEMES FOR ATMOSPHERIC MODELS

Different PBL schemes are described in this chapter ranging from very simple drag laws to formulations based on the turbulence kinetic energy equation. Since the geostrophic drag laws are becoming less and less popular, they will only be described briefly. Most attention will be paid to (vertical) grid point parametrizations with simple closure for the exchange coefficient as they are the most popular ones.

3.1 Geostrophic transfer laws

Geostrophic transfer laws can be used to introduce some effects of surface fluxes in models that have hardly any or no levels in the boundary layer. They are based on boundary layer similarity for the steady state boundary layer. A relation is assumed between the model variables at the lowest model level and the fluxes at the surface, where the lowest model level is assumed to be at the top of the boundary layer or above the boundary layer. Such an approach makes only sense in models with low resolution near the surface. The simplest form of a bulk transfer law expresses the surface fluxes of momentum, heat and moisture into the model variables U_G, V_G, θ_G, q_G above the boundary layer and surface values θ_s and q_s in the following way:

$$(\overline{u'w'})_0 = -C_M |\mathbf{U}_G| U_G \tag{74}$$

$$(\overline{v'w'})_0 = -C_M |\mathbf{U}_G| V_G \tag{75}$$

$$(\overline{w'\theta'})_0 = -C_H |\mathbf{U}_G| (\theta_G - \theta_s) \tag{76}$$

$$(\overline{w'q'})_0 = -C_Q |\mathbf{U}_G| (q_G - q_s) \tag{77}$$

The index G has been used here to indicate variables above the boundary layer; for wind it can be thought of as geostrophic wind. The constants C_M, C_H and C_Q are chosen from field data or adjusted on the basis of model performance. Different values can be chosen for land and sea. Advantages of this scheme are: (i) the scheme is very simple and (ii) it is a first order approximation for the influence of surface fluxes. Disadvantages are: (i) the scheme does not have a diurnal cycle, (ii) there are no effects of stability, (iii) the empirical coefficients are very uncertain, (iv) there are no forecast products in the PBL and (v) the physics of the PBL is poorly represented.

A second "bulk" scheme, which is very similar to the first one, introduces stability effects in the transfer coefficients C_M, C_H and C_Q in accordance with the similarity theory discussed in Section 2.3.

$$C_M = C_H = C_Q = \left[\frac{1}{k} \ln\left(\frac{u_*}{f z_{0M}} \right) - \frac{A}{k} \right]^{-2} \tag{78}$$

$$\text{where } A = A\left(\frac{u_*}{fL} \right), \text{ or } A = A\left(\frac{h}{L} \right), \tag{79}$$

$$\text{and } u_* = \left\{ (\overline{u'w'})_0^2 + (\overline{v'w'})_0^2 \right\}^{\frac{1}{2}}, L = \frac{-u_*^3}{k\left(\frac{g}{\theta_v} \right)(\overline{w'\theta_v'})_0}. \tag{80}$$

The constant A depends on stability and is the same one as in Eq. (63). Experimental data on A is shown in Fig. 14 (Clarke and Hess 1974). This formulation is slightly more realistic than the first one but is very much limited to the simple situations, for which the transfer laws are known. However, with an appropriate land surface scheme for the surface temperature θ_s and surface moisture q_s, this scheme allows for diurnal variation of the surface drag through the stability dependence of parameter A. The more complicated case of the unsteady PBL, cases with strong advection, baroclinic or inversion capped PBL's are not expected to be well captured by bulk transfer laws.

3.2 Integral models (slab, bulk models)

In integral models the entire boundary layer is characterized by a limited number of parameters (e.g. PBL depth, mean velocity, mean temperature etc.). Prognostic equations are derived for these PBL characteristics rather than for the basic variables. The main advantage is that the PBL does not have to be resolved by the vertical layer structure of the model.

The basic assumption for integral models is that a similarity form exists for the model variables e.g. for potential temperature:

$$\frac{\theta - \theta_G}{\theta_*} = f\left(\frac{z}{h}\right), \tag{81}$$

where θ_* is a temperature scale and h the boundary-layer height. When the form of f is known from field experiments, Eq. (81) can be substituted in the equations of motion and integrated from the surface to $z = h$. The resulting differential equations for θ_* and h describe the entire PBL without resolving it explicitly in the vertical.
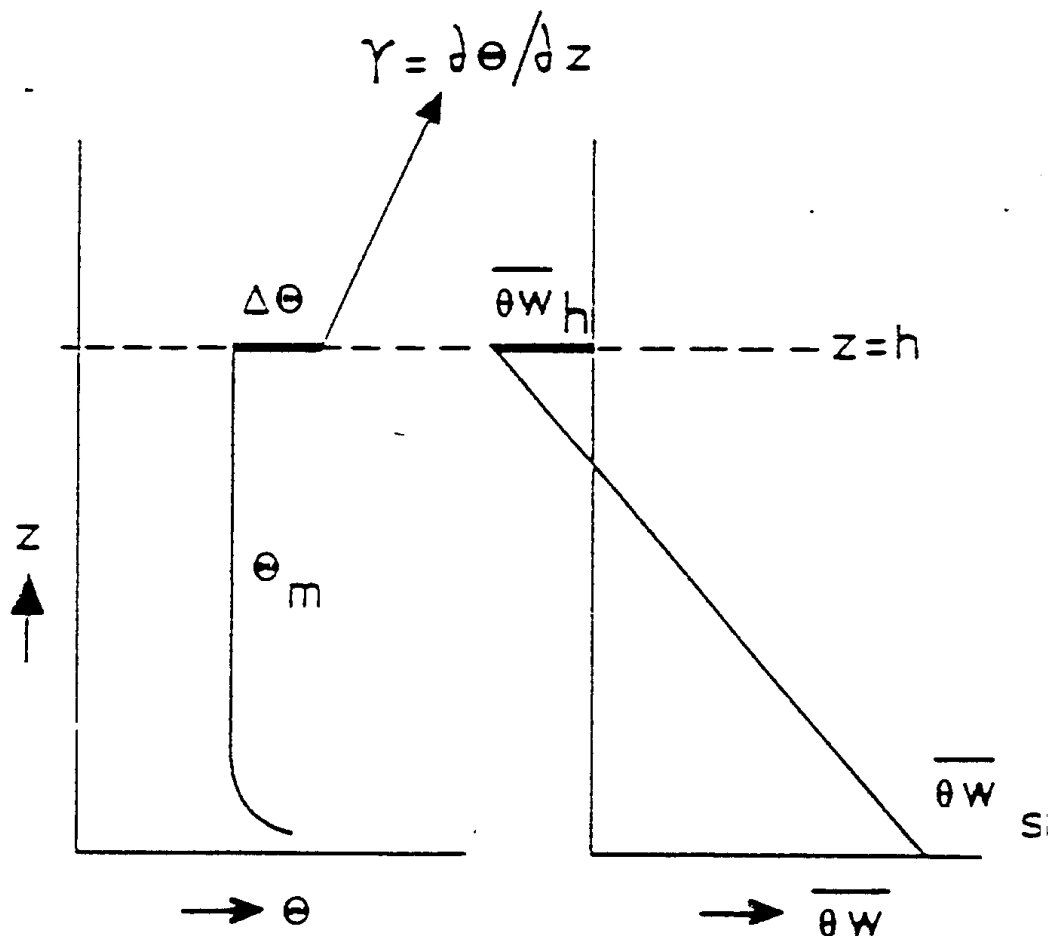

Figure 20. Schematic profiles of θ and $\overline{\theta' w'}$ in a mixed layer model.

This approach is illustrated with help of a slab model for the convective boundary layer (mixed layer). In the mixed layer the turbulent exchange is sufficiently strong to make the profiles of wind, potential temperature and specific

humidity approximately uniform in the bulk of the boundary layer (the simplest possible expression for f). The near surface part shows gradients, but the surface layer is relatively shallow and does therefore not contribute significantly to the budgets of the total boundary layer. Here we limit to the budget of potential temperature because it is the main quantity that feeds back to the dynamics of the mixed layer. Quantity θ_m represents the potential temperature in the bulk of the mixed layer and its time evolution is determined by heat fluxes at the surface and the top of the mixed layer (Fig. 20 illustrates the temperature structure of the well mixed layer; see Driedonks and Tennekes, (1984)):

$$h\frac{d\theta_m}{dt} = (\overline{w'\theta'})_0 - (\overline{w'\theta'})_h \,, \tag{82}$$

$$\frac{dh}{dt} = w_e + w_L \,, \tag{83}$$

$$\frac{d\Delta\theta_m}{dt} = \gamma w_e - \frac{d\theta_m}{dt} \,, \tag{84}$$

$$(\overline{w'\theta'})_h = -w_e\Delta\theta \,. \tag{85}$$

In these equations $\Delta\theta_m$ represents the potential temperature jump at the top of the boundary layer, w_e the entrainment velocity, w_L the large scale resolved vertical velocity at height h, and γ the stable lapse rate above the mixed layer. Equations (82)–(85) describe the energy budget, the height and the temperature step at the top of the mixed layer and have a simple physical interpretation. The rate of change of the energy of the mixed layer is proportional to the difference of heat flux at the surface and the top (Eq. (82)); the height change of the mixed layer with respect to the large scale ascent or descent is by definition the entrainment velocity (Eq. (83)); the temperature step at $z = h$ changes due to temperature changes of the mixed layer and due a shift of the mixed layer with respect to the stable lapse rate (Eq. (84)); and the entrainment heat flux is the amount of air that is entrained times the temperature jump (Eq. (84)). This set of equations is not closed; it has to be supplemented by equations for the surface fluxes and by an entrainment assumption. The surface fluxes can be obtained by using surface layer formulations as discussed in Section 2.4. For the heat flux, Eq. (67) can be used with z somewhere in the mixed layer and $\theta = \theta_m$.

To parametrize the entrainment we consider the equation for turbulent kinetic energy:

$$\frac{\partial E}{\partial t} = \underbrace{-\overline{u'w'}\frac{\partial U}{\partial z} - \overline{v'w'}\frac{\partial V}{\partial z}}_{(I)} \quad \underbrace{+\frac{g}{\rho_0}\overline{w'\theta_v'}}_{(II)}$$
$$\underbrace{+\frac{\partial}{\partial z}\left(\overline{E'w'} + \overline{\frac{p'w'}{\rho}}\right)}_{(III)} \quad \underbrace{-\varepsilon}_{(IV)} \quad . \tag{86}$$

This equation describes the balance between shear production (I), buoyancy production or destruction (II), transport by turbulent velocity and pressure fluctuations (III) and dissipation (IV). The order of magnitude of the different terms typical for the entire mixed layer depth can be expressed in terms of velocity and length scales characteristic for the mixed layer:

I: u_*^3/h

II: $(g/\theta_v)(\overline{w'\theta_v'})_h + w_*^3/h$

$$\text{III: } (u_*^3 + w_*^3) / h$$

$$\text{IV: } (u_*^3 + w_*^3) / h$$

These estimates have been made by assuming a single length scale h as turbulence length scale and for the estimation of the derivatives and by assuming that the turbulent fluctuations have magnitude w_* (see (57) for its definition). It is important to realize here what the mechanism of entrainment is. The energy is produced by shear and buoyancy in the bulk of the mixed layer. Most of the energy is transferred to smaller and smaller scales and ultimately converted into heat by viscous dissipation. Some of it is diffused upwards by the turbulent motion itself (e.g. thermals) and penetrates into the inversion where it is destroyed by the negative buoyancy (Fig. 21 illustrates the energy budget of the mixed layer). So the entrainment at the top of the mixed layer is fed by upward diffusion of turbulent kinetic energy produced in the bulk of the mixed layer.

Since the dominant terms are of the order of w_*^3 / h, it is to be expected that the buoyancy flux at $z = h$ is also proportional to this quantity. An obvious closure therefore is:

$$(\overline{w'\theta_v'})_h = C_e (\overline{w'\theta_v'})_0 \tag{87}$$

where the "entrainment" constant C_e is determined from experimental data. The numerical value of C_e is about 0.2 (Driedonks and Tennekes 1984).

The advantages of integral models are obvious: (i) they are relatively simple, (ii) they do not rely on vertical resolution and (iii) they are physically realistic for simple cases as the mixed layer. Disadvantages are: (i) this type of models is difficult to implement as they involve a moving boundary condition (the top of the boundary layer) for the atmosphere above the PBL, (ii) the similarity profiles are less obvious for e.g. the stable boundary layer and virtually unknown for more complicated boundary layers as e.g. the baroclinic or cloudy boundary layer and (iii) the transition between different scaling regimes (e.g. from unstable to stable) are difficult to handle. For mixed layer models in particular it has to be added that they perform very well for a well mixed quantity as potential temperature, but quite poorly for less well mixed quantities as momentum and specific humidity.

Because of the technical complications of having a moving lower boundary condition in a forecast model, Deardorff (1972) proposed to combine the integral boundary layer approach with a fixed vertical grid structure. This scheme was specially designed for GCM's with poor vertical resolution. The diagnosed boundary layer height can be below and above the lowest model level (Fig. 22). The boundary layer height can be seen as an additional model level at the height where the structure of the atmosphere changes drastically. After every time step, with the PBL scheme the grid points inside the boundary layer are adjusted to the mixed-layer profile.
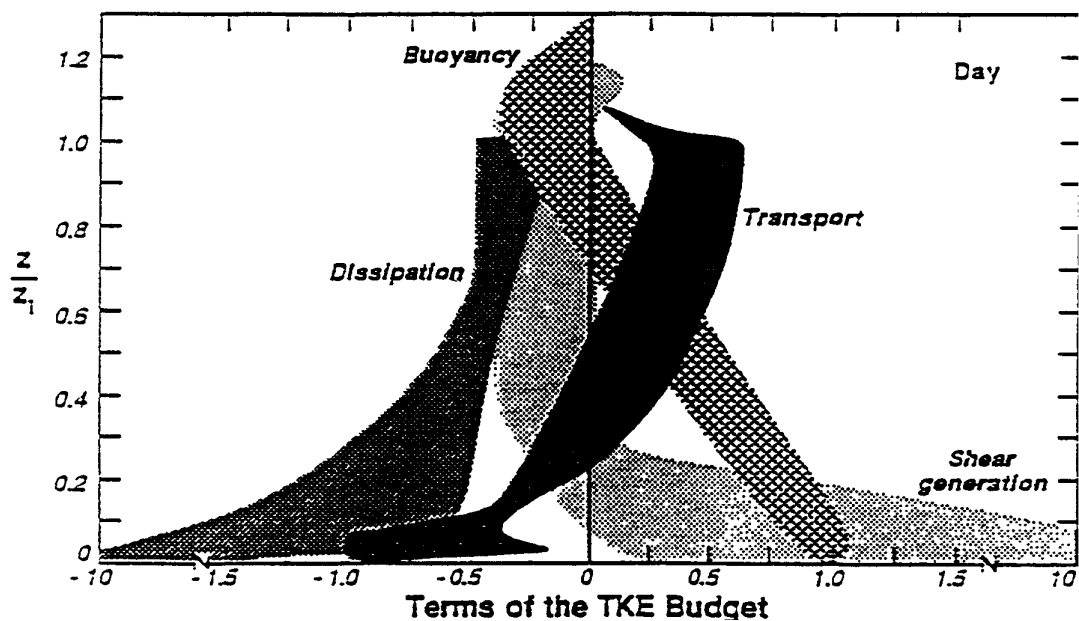
Figure 21. Normalized terms of the turbulence kinetic energy equation. The normalization is on w_*^3/h . (Fig. 5.4 from Stull 1988)
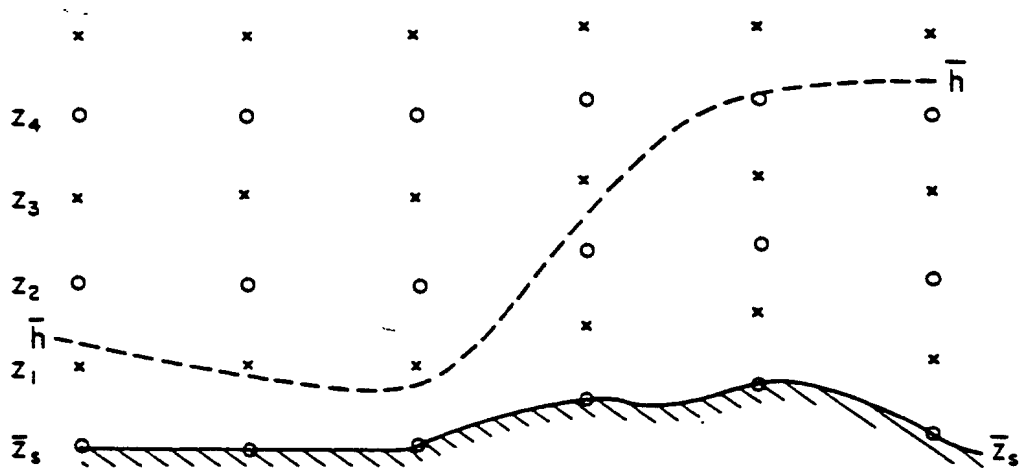
Figure 22. Grid point structure in Deardorff's (1972) PBL model.

3.3 Grid point models with K-closure

General description

A fairly simple closure for models that resolve the boundary layer explicitly, is the K-type closure. In analogy with molecular diffusion, it is assumed that the fluxes are proportional to the gradients (Louis, 1979):

$$\overline{u'w'} = -K_M \frac{\partial U}{\partial z} \;\;,\;\; \overline{v'w'} = -K_M \frac{\partial V}{\partial z} \;\;,$$ (88)

$$\overline{w'\theta'} = -K_H \frac{\partial \theta}{\partial z} \;\;,\;\;\;\;\; \overline{w'q'} = \;\;\; K_H \frac{\partial q}{\partial z} \;\;.$$ (89)

The exchange coefficient K is not a property of the fluid as in molecular diffusion, but depends on the flow. Surface layer similarity provides the formulation for K near the surface (i.e. in the lowest model layer):

$$K_M = \frac{l^2}{\phi_M^2} \left| \frac{dU}{dz} \right| \;\;,\;\;\;\; K_M = \frac{l^2}{\phi_M \phi_H} \left| \frac{dU}{dz} \right| \;\;,$$ (90)

where $l = kz$. Use of the same expression in the outer layer (above the lowest model level), would be consistent with the ideas of local scaling (Section 2.2) for the stable boundary layer, provided that ϕ_M, ϕ_H and ϕ_Q are proportional to z for large z/L. In this way the length scale z drops out for large z. Two problems arise from such a simple extension of surface layer similarity both related to the lack of an upper bound to l: (i) the diffusion coefficient becomes very large in neutral situations and (ii) with ϕ_M different from ϕ_H in stable situations (necessary for reasons to be explained later), local scaling breaks down and l remains an essential part of the parametrization. To limit the length scale Blackadar (1962) proposed the following expression:

$$\frac{1}{l} = \frac{1}{kz} + \frac{1}{\lambda}$$ (91)

This formulation obeys surface layer similarity and is consistent with local scaling for the stable boundary layer. The only additional parameter that has been introduced is the asymptotic length scale λ, which is often the same for momentum and heat. The idea is that the turbulence length scale is limited by the boundary layer height. In some parametrizations $\lambda \sim u_*/f$ or $\lambda \sim h$, where h is a diagnosed boundary layer height. Since the results are not very sensitive to the exact value of l, this parameter is often chosen constant.

Expressions (90) contain ϕ which depends on z/L in the surface layer and therefore on the surface fluxes. Above the surface layer the ϕ-functions depend on l/kL instead of z/L to be consistent with the ideas of local scaling. An inconvenient aspect of Eq. (90) is that it contains fluxes which makes the closure an implicit one. To find an explicit closure we substitute the closure assumptions in the definition of the Obukhov length and obtain:

$$Ri = \frac{g}{\theta_v} \frac{\dfrac{d\theta_v}{dz}}{\left| \dfrac{dU}{dz} \right|^2} = \frac{l}{kL} \frac{\phi_H}{\phi_M^2}$$ (92)

This is a relation between the gradient Richardson number and l/L which can be solved numerically when the ϕ-functions are specified. Instead of closure assumption (90) it is much more efficient to specify stability functions that depend on the Richardson number because then we have the fluxes explicitly in terms of model variables:

$$K_M = l^2 F_M \left| \frac{dU}{dz} \right| \;\;,\;\;\;\; K_H = l^2 F_H \left| \frac{dU}{dz} \right| \;\;,$$ (93)

where $F_M = F_M(Ri)$ and $F_H = F_H(Ri)$, and by definition: $F_M = \phi_M^{-2}$, $F_H = (\phi_M \phi_H)^{-1}$.

Equation (93) is the closure as it is actually used in many models. The functions F_M and F_H are specified as analytical functions of Ri or are tabulated. In both cases they are derived from empirical data on ϕ_M and ϕ_H which are functions of z/L (or l/kL), so the independent variable has been transformed from z/L (or l/kL) to Ri with Eq. (92).

```
       19          31
      level       level
      model       model
 z = 3890        1800     ─────────────────────── U, V, T, q
                          -----------------------
 z = 2200        1360     ─────────────────────── U, V, T, q
                          -----------------------
 z = 1400         970     ─────────────────────── U,- V, T, q
                          -----------------------
 z =  810         640     ─────────────────────── U, V, T, q
                          -----------------------
 z =  395         356     ─────────────────────── U, V, T, q
                          -----------------------
 z =  150         150     ─────────────────────── U, V, T, q
                          -----------------------
 z =   33          33     ─────────────────────── U, V, T, q
 z =   z_o         z_o    ////////////////////////  0, 0, T_s, q_s
```
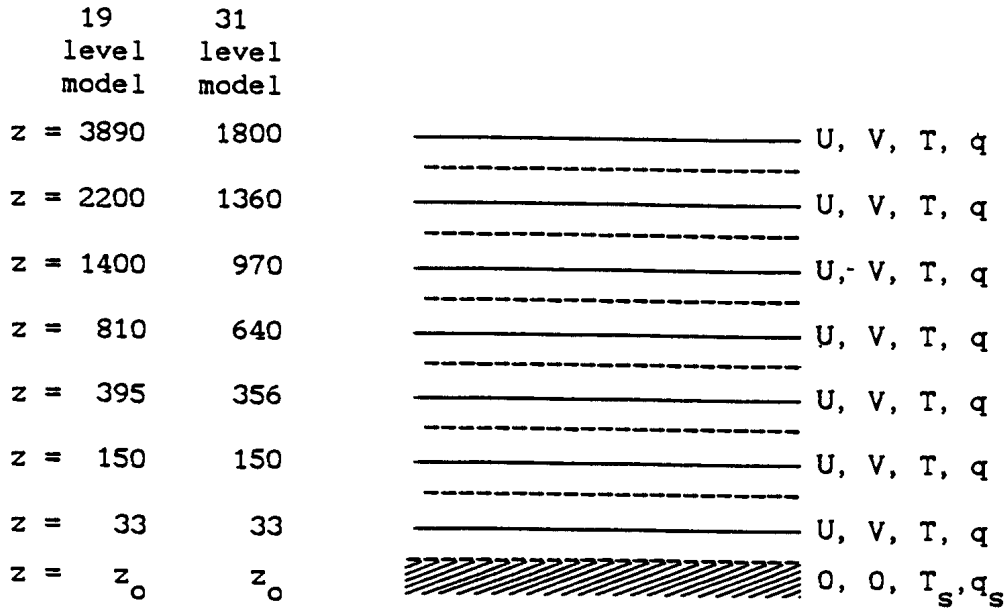
Figure 23. The vertical grid structure near the surface in the ECMWF model (19-level version and 31-level version). Solid lines represent model levels; dashed lines are flux levels.

The gradients as needed in the closure assumption are computed from the grid point values by means of a finite difference approximation (cf. Fig. 23). A staggered grid is used with flux levels between the full model levels. A simple finite difference approximation (assuming linearly interpolated profiles between model levels) is not accurate near the surface, where the profiles of wind temperature and moisture show pronounced non-linear behaviour particularly near the surface. To derive a finite difference form for the surface layer we assume that the flux is constant with height and integrate the closure assumptions from the surface to $z = z_1$ where z_1 is the height of the lowest model level. This results in the usual surface layer profiles:

$$U_1 = \frac{\tau_{x0}}{\rho k u_*}\left[\ln\left(\frac{z_1}{z_{0M}} + 1\right) - \Psi_M\left(\frac{z_1}{L}\right)\right] \tag{94}$$

$$V_1 = \frac{\tau_{y0}}{\rho k u_*}\left[\ln\left(\frac{z_1}{z_{0M}} + 1\right) - \Psi_M\left(\frac{z_1}{L}\right)\right] \tag{95}$$

$$\theta_1 - \theta_s = \frac{(-\overline{w'\theta'})_0}{k u_*}\left[\ln\left(\frac{z_1}{z_{0H}} + 1\right) - \Psi_H\left(\frac{z_1}{L}\right)\right] \tag{96}$$

$$q_1 - q_s = \frac{(-\overline{w'q'})_0}{k u_*}\left[\ln\left(\frac{z_1}{z_{0Q}} + 1\right) - \Psi_H\left(\frac{z_1}{L}\right)\right] \tag{97}$$

These expressions can be interpreted as an exact finite difference representation of the lowest model layer. Unfortunately it is an implicit formulation as it contains z/L. Again we can relate the "flux-stability parameter" z/L to the bulk Richardson number Ri_b:

$$Ri_b = \frac{g}{\theta_v} \frac{z_1(\theta_{v1} - \theta_{v0})}{|\mathbf{U}_1|^2} \tag{98}$$

$$= \frac{z_1}{L} \frac{\ln\left(\frac{z_1}{z_{0H}} + 1\right) - \Psi_H\left(\frac{z_1}{L}\right)}{\left[\ln\left(\frac{z_1}{z_{0M}} + 1\right) - \Psi_M\left(\frac{z_1}{L}\right)\right]^2} \tag{99}$$

This equation relates Ri_b to z_1/L, z_1/z_{0H} and z_1/z_{0M}. For computational efficiency the stability functions are usually represented in terms of the bulk Richardson number Ri_b. The surface fluxes of momentum (τ_x and τ_y), heat (H) and water vapour (E) are expressed in model variables at the lowest model level in the following way:

$$\frac{\tau_x}{\rho} = C_M|\mathbf{U}_1|U_1 \tag{100}$$

$$\frac{\tau_y}{\rho} = C_M|\mathbf{U}_1|V_1 \tag{101}$$

$$-\frac{H}{\rho c_p} = C_H|\mathbf{U}_1|(\theta_1 - \theta_s) \tag{102}$$

$$-\frac{E}{\rho} = C_Q|\mathbf{U}_1|(q_1 - q_s) \tag{103}$$

where

$$C_M = C_{MN}F_M\left(Ri_b, \frac{z_1}{z_{0M}}, \frac{z_1}{z_{0H}}\right) \tag{104}$$

$$C_H = C_{QN}F_Q\left(Ri_b, \frac{z_1}{z_{0M}}, \frac{z_1}{z_{0H}}\right) \tag{105}$$

$$C_Q = C_{MN}F_M\left(Ri_b, \frac{z_1}{z_{0M}}, \frac{z_1}{z_{0H}}\right) \tag{106}$$

With the neutral transfer coefficients defined as:

$$C_{MN} = \left[\frac{k}{\ln\left(\frac{z_1}{z_{0M}}\right)}\right]^2 \tag{107}$$

$$C_{\text{HN}} = \left[\frac{k}{\ln\left(\frac{z_1}{z_{0\text{H}}}\right)} \right]^2 \tag{108}$$

$$C_{\text{QN}} = \left[\frac{k}{\ln\left(\frac{z_1}{z_{0\text{Q}}}\right)} \right]^2 \tag{109}$$

The closure assumptions are hidden now in the empirical functions of the Richardson number, which are never measured directly. The reason is that they depend on the surface conditions (surface roughness lengths) which makes it difficult to determine them directly from data. Experiments, however, do provide data on the ϕ or Ψ functions. From there we can derive numerically the F functions for different surface roughness lengths and make an empirical fit to be used in the forecast model. However the F functions (104)–(106) depend on three different parameters and it can be difficult to obtain simple empirical expressions that are accurate for all possible vales of the parameters. In many models the three roughness lengths are the same which reduces the number of independent parameters to 2, but the empirical functions can still be fairly inaccurate as will illustrated subsequently.

The stability functions

The main difficulty with K-closure is the specification of the stability functions. Louis et al. (1982) give an overview of how these function have evolved in the operational ECMWF model as the result of adjustments on the basis physical arguments and model performance. The functions that have been used since December 1981 are (Louis et al. 1982):

$$F_{\text{M}} = 1 - \frac{2bRi_0}{1 + C_h(-Ri_0)^{1/2}} \quad \text{for} \quad Ri_0 < 0 \tag{110}$$

$$F_{\text{H}} = 1 - \frac{3bRi_0}{1 + C_h(-Ri_0)^{1/2}} \quad \text{for} \quad Ri_0 < 0 \tag{111}$$

$$F_{\text{M}} = \frac{1}{1 + 2bRi_0(1 + dRi_0)^{-1/2}} \quad \text{for} \quad Ri_0 > 0 \tag{112}$$

$$F_{\text{H}} = \frac{1}{1 + 3bRi_0(1 + dRi_0)^{1/2}} \quad \text{for} \quad Ri_0 > 0 \tag{113}$$

where $b = 5$, $c = 5$, and $d = 5$, and

$$C_h = 3bc \frac{k^2\left(1 + \frac{z_1}{z_{0\text{M}}}\right)^{1/2}}{\left[\ln\left(1 + \frac{z_1}{z_{0\text{M}}}\right)\right]^2} \quad \text{in the surface layer, and}$$

$$C_h = \frac{l^2}{3z^2} \quad \text{above the surface layer.}$$

Extensive diagnostics of operational forecasts has shown that the diffusion was too strong in the middle and upper troposphere, where the jet stream was partially smeared out by the action of the vertical diffusion scheme. It was therefore decided to make a rough estimate of the boundary layer height and to switch off the scheme above the boundary layer in stable situations. This change was introduced operationally in January 1988. The poor performance of the scheme above the boundary layer can be attributed to the shape of the stability function in the Richardson number range of 0.1 to 1.

An alternative form of the stability functions (the $F(Ri)$ functions) can be derived from the ϕ functions (34)–(35) in unstable situations and (39)–(40) in stable flow. We will call them the M.O. functions. The comparison of the stability functions is shown in Fig. 24 . We see that for positive Richardson numbers the functions derived from ϕ_M and ϕ_H depend on the surface roughness length. The most pronounced difference above the surface layer is that the M.O. functions give much smaller values above $Ri = 0.1$ in comparison to the Louis et al. (1982) functions.

It should be realized that the shape of the stability functions is subject to an ongoing debate (Hogstrom 1988). The difficulties originate from limitations in the concept of local diffusion and from uncertainties in the experimental data. An example of the first difficulty is the unstable or convective boundary layer where the diffusion is not local. The reason that a local scheme still performs reasonably well is that the coefficients become large and therefore the profiles virtually uniform irrespective of the exact magnitude of the diffusion coefficients. For quantities that are not well mixed in the convective boundary layer as e.g. moisture or wind in a baroclinic PBL, a local scheme is expected to be less appropriate. A second example of the same problem is diffusion in stably stratified flow in the intermittent regime. Local scaling works fairly well in the fully turbulent regime up to Richardson numbers of 0.2. Beyond 0.2, turbulence becomes intermittent and the diffusive characteristics are not well understood. Also wave-turbulence interaction is a relevant process in this range. The reported magnitude of the diffusion coefficients in clear-air turbulence (Richardson numbers between 0.2 and 1) varies by and order of magnitude from one study to the other (Kennedy and Shapiro 1980; Ueda et al. 1981; Kondo et al. 1978; Nieuwstadt 1984; Kim and Mahrt 1991). The shape of functions ϕ_M and ϕ_H as expressed by Eqs. (39)–(40) is reasonably well documented (see Beljaars and Holtslag 1991) for weak and moderate stability. The ratio ϕ_M / ϕ_H, however, is inspired by the idea that this ratio should become proportional Ri for large Richardson numbers (see Eq. (92)). This particular asymptotic behaviour is much less documented, but is quit relevant to the transformation from z/L to Ri in Eq. (92). Another parameter that determines to a large extent the diffusion in the clear-air turbulence domain is the asymptotic length scale λ. A simple parametrization strategy is to select stability functions which are reasonably well documented from $Ri = 0$ to $Ri = 0.2$, apply physical constraints for large Richardson numbers as in Eqs. (39)–(40) and adjust λ to obtain reasonable diffusion coefficients in the clear air turbulence domain e.g. on the basis of data by Kennedy and Shapiro (1980).

One column simulations

To illustrate the characteristics of K-closure, a single column version of the vertical diffusion scheme has been integrated over 9 hours with constant geostrophic forcing and constant forcing from the surface. In this way, a nearly steady state is obtained. The selected forcing is a constant geostrophic wind of 10 m/s and a constant surface heat flux. The surface roughness length is 0.1 m. Fig. 25 shows the A and B parameters in the drag law of Eqs. (63) –(64) as the result of the parametrization with Louis et al. (1982) stability functions and with the M.O. stability functions. The comparison with empirical data shows little difference; the main difference is that the M.O scheme covers a much larger dimensionless stability range than the Louis et al. scheme for the same range of surface fluxes. The difference between the two schemes is more obvious in the Figs. 26 and 27 for a downward heat flux of 20 W/m. First of all we sea that the surface stress is much smaller with the M.O. scheme and that the PBL is less deep. Boundary layer heights with the M.O. scheme are much more realistic and compare much better with data as for instance expressed by the empirical equilibrium heights proposed by Zilitinkevich (1972) or observations by Nieuwstadt (1981).

With a relatively low number of grid points in the PBL, significant discretization errors can be expected. The shallow stable boundary layer could be particularly affected as it is only resolved by two or three model levels. The effect of resolution on the structure of the stable boundary layer is shown in Fig. 28 , where a simulation with the 19-level model resolution is compared to a simulation with three times as many levels. We see that the results are very similar and that the low resolution simulation is fairly accurate. The unexpected robustness of the numerical scheme is related to the treatment of the surface layer where a considerable part of the shear and temperature gradients are concentrated. In the surface layer the scheme uses the integral profile functions (94)–(97) as a bulk formulation rather than a finite difference form. It is known from other applications that the integral profile functions are quite accurate also when extrapolated outside the surface layer (VanWijk et al. 1990).
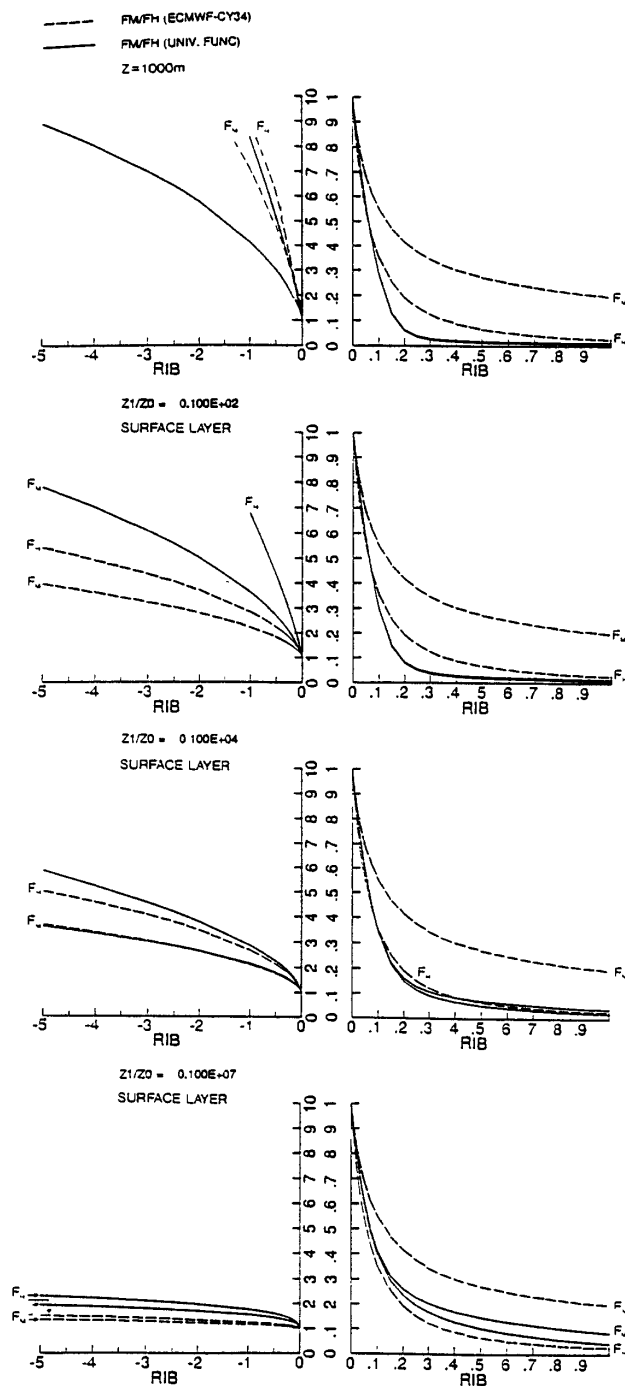
Figure 24. Stability functions according to Louis et al. (1982) and derived from the universal φ-functions (M.O. scheme) above the surface layer and for different surface roughness lengths in the surface layer.
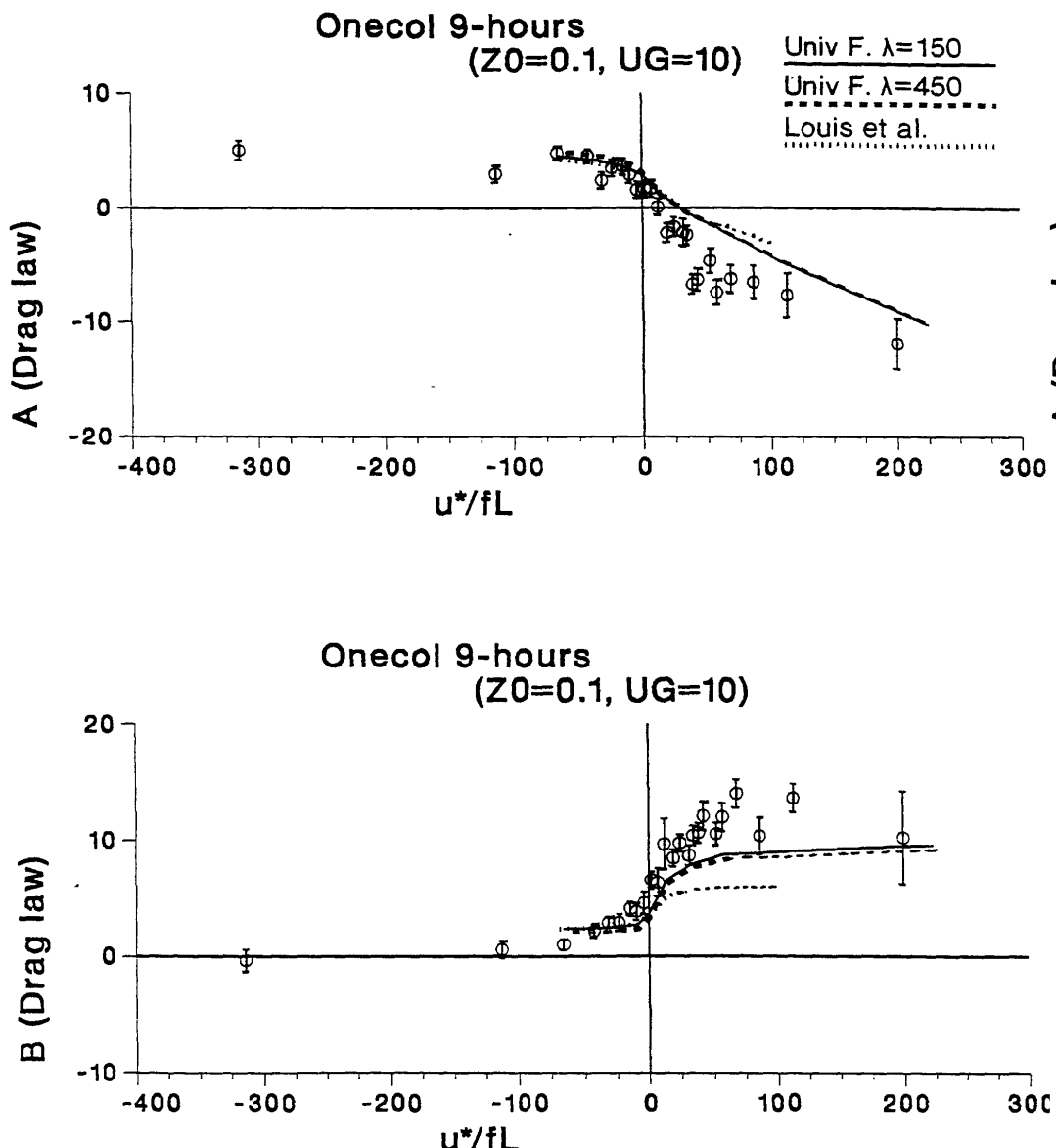
Figure 25. *A* and *B* parameters in the geostrophic drag law as simulated with the Louis et al. (1982) functions and the M.O. stability functions.
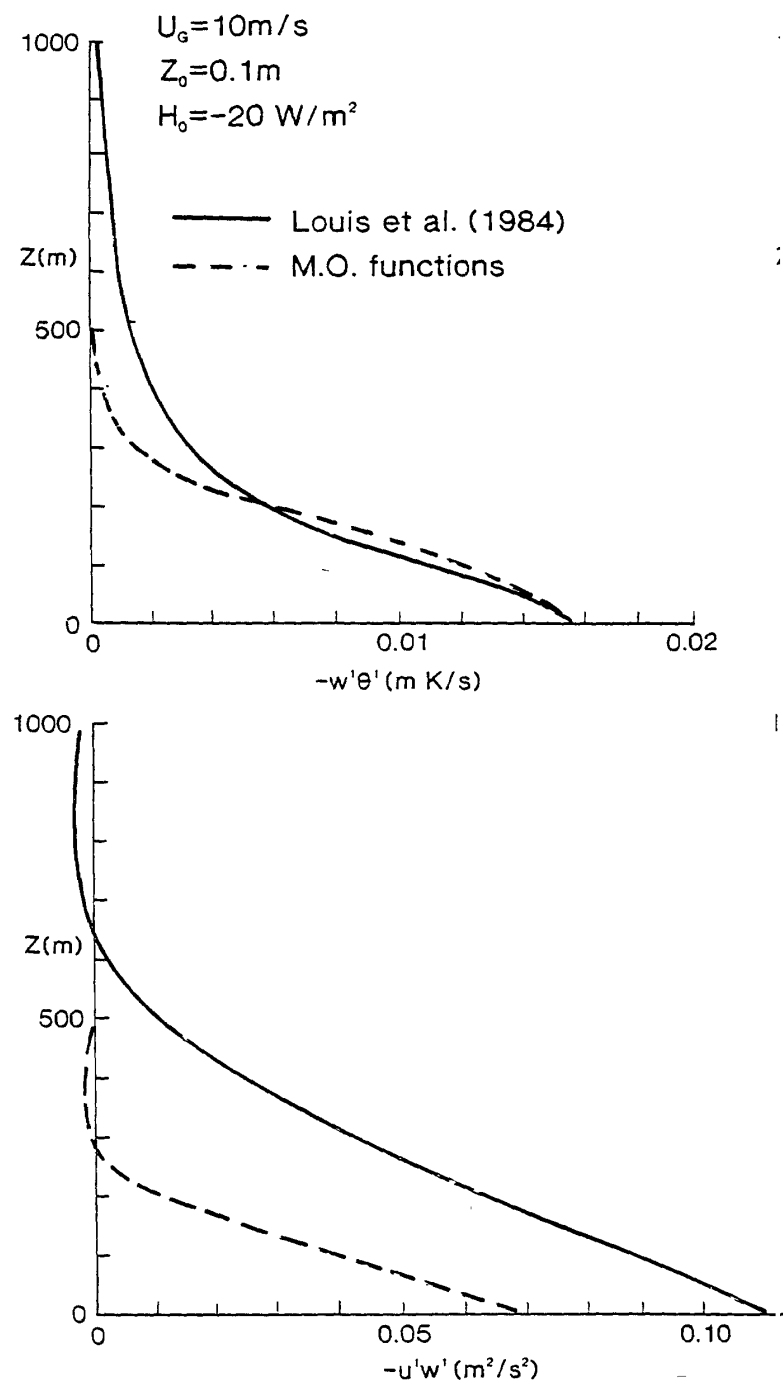
Figure 26. Flux profiles in the stable boundary layer with Louis et al. (1982) functions (solid) and iteratively obtained functions from the M.O. ϕ-functions (dashed).
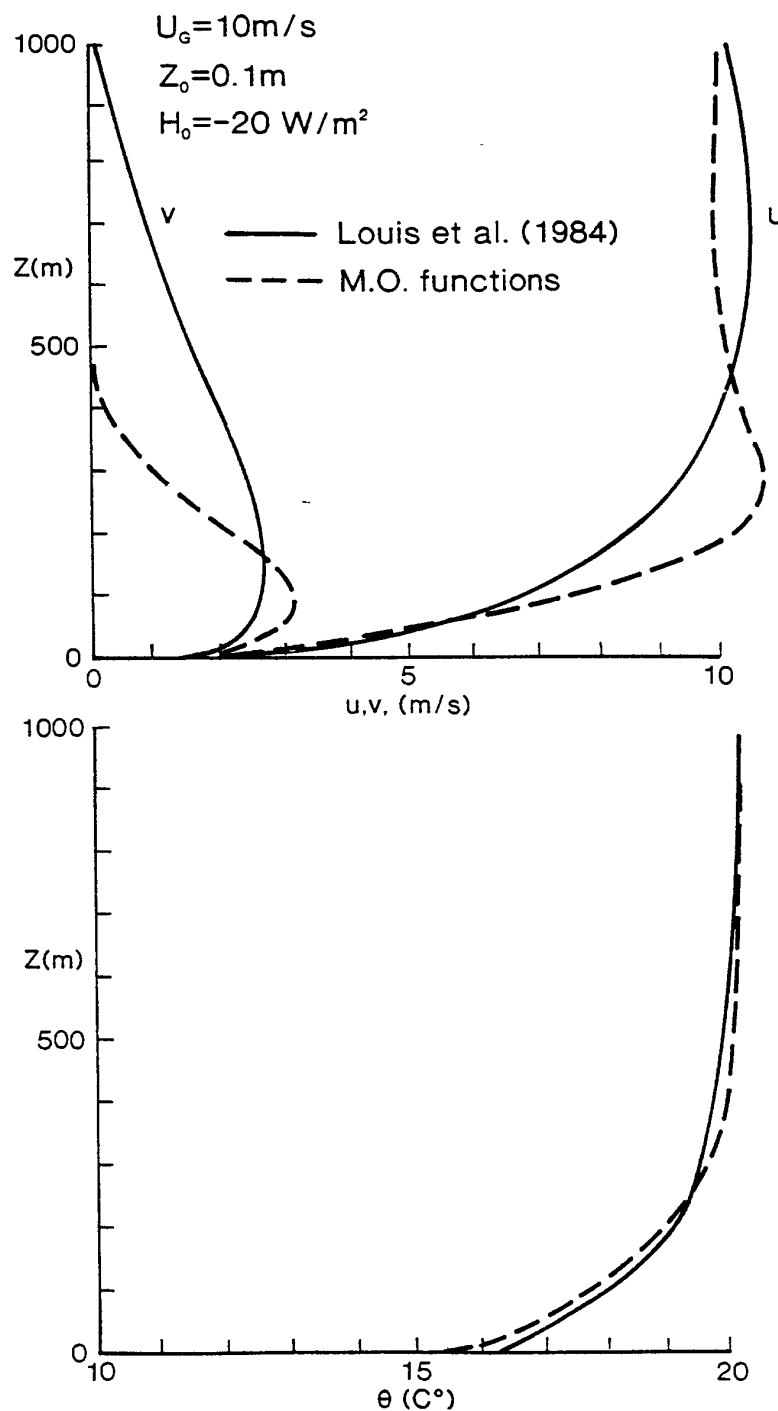
Figure 27. As Fig. 25 , but for wind and temperature profiles
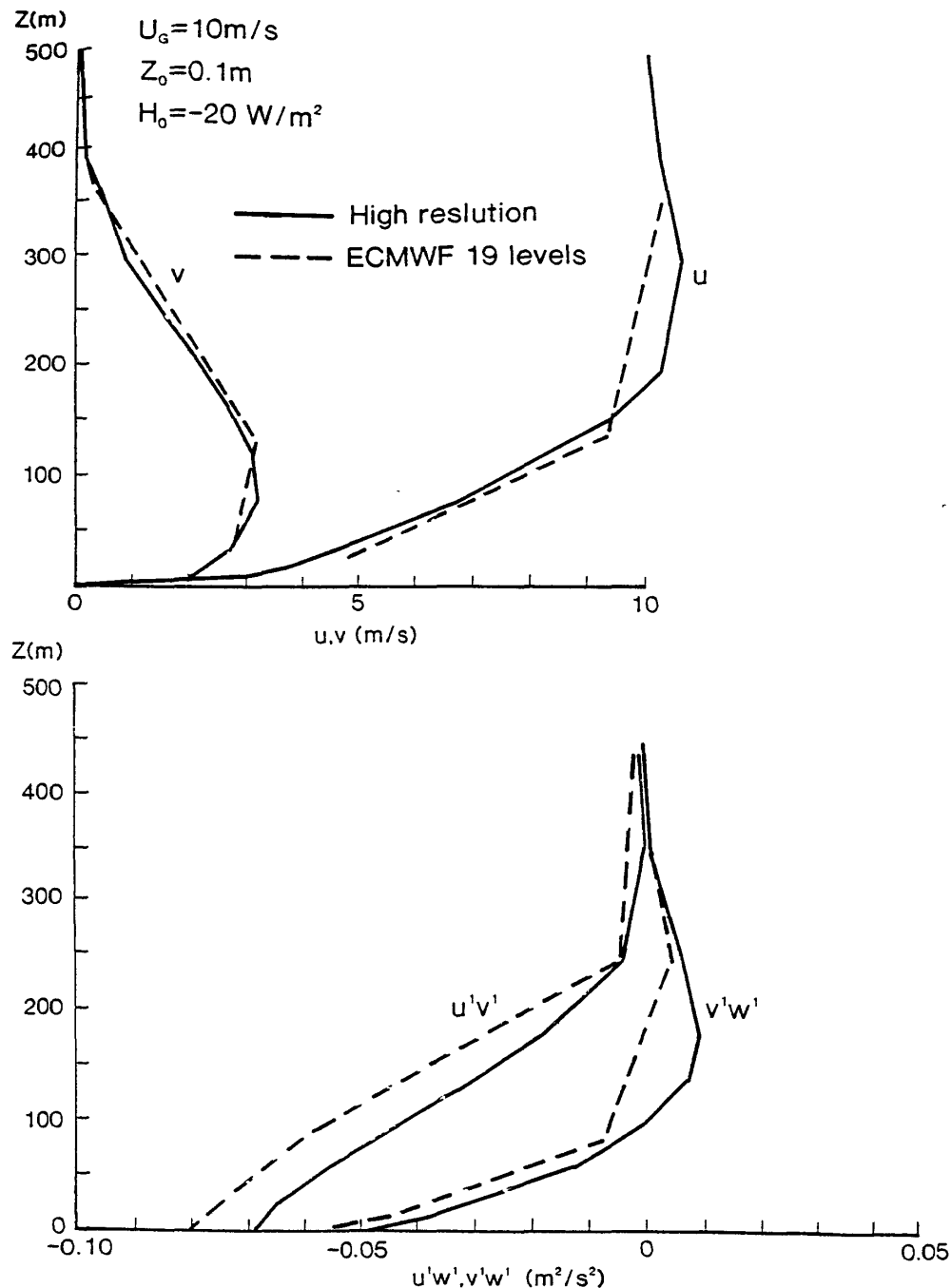
Figure 28. Illustration of resolution dependence of a 9-hour integration for the stable boundary layer in one column mode.

Concluding remarks

The advantage of K-closure with local expressions for the diffusion coefficients is that it is fully consistent with the grid point formulation of the model and that the same scheme can be used for stable, unstable, baroclinic, land, sea

etc. A disadvantage is that a number of model levels are needed to resolve the boundary layer. On the other hand, it is quite remarkable that the scheme performs fairly well with 2 levels in a shallow stable boundary layer. The reason is that the surface layer approximation is exact in the sense that the surface layer profile between the surface and the lowest model level is represented exactly. The resolution is only needed to obtain a reasonable shear stress profile, but flux profiles are generally fairly linear as function of height and can be represented with a few points only. Proper resolution is needed however to resolve inversions. Since the position of the inversion is variable, good resolution is needed trough out the lower troposphere (Beljaars 1991). This is obviously a disadvantage compared to mixed layer models where a dedicated model variable exists to keep track of the inversion height. Another disadvantage is that the closure is local and does not account for the "integral" aspects of e.g. the convective boundary layer. Although the physics of the convective boundary layer is not well described with local closure, this is not a real problem in practice because a well mixed layer is always produced when the exchange coefficients are sufficiently large. Local closure has its limitations of course as it does not describe aspects as counter-gradient fluxes, not well-mixed parameters etc. The main disadvantage of local closure is that it does not describe entrainment at the top of the mixed layer, because the non-local mechanism of entrainment is not represented at all by a local closure scheme. With local closure the entrainment rate is generally zero as the local closure produces very small exchange coefficients in stable stratification.

In summary we can say the K-type closure is very realistic for the stable PBL if the resolution is sufficient; also in the unstable boundary layer, well-mixed quantities are well represented, but entrainment is not modelled at all.

3.4 *K*-profile closures

An interesting closure which has been proposed for low resolution models is the K-profile closure (see Troen and Mahrt 1986 and Holtslag et al. 1990). The exchange coefficients are not expressed in local gradients but as integral profiles for the entire PBL. The boundary layer height and the surface fluxes are used as scaling parameters. Also counter gradient terms are included in the formulation. The exchange coefficients are prescribed as follows for the stable boundary layer and the unstable surface layer ($z / h < 0.1$):

$$\overline{u'w'} = K_{\mathrm{M}}\frac{\partial U}{\partial z} \ , \quad \overline{v'w'} = K_{\mathrm{M}}\frac{\partial V}{\partial z} \ , \tag{114}$$

$$\overline{w'\theta'} = K_{\mathrm{H}}\frac{\partial \theta}{\partial z} \ , \quad \overline{w'q'} = K_{\mathrm{H}}\frac{\partial q}{\partial z} \ , \tag{115}$$

$$K_{\mathrm{M}} = k w_{\mathrm{s}} z \left(1 - \frac{z}{h}\right)^2 \tag{116}$$

$$K_{\mathrm{H}} = k w_{\mathrm{s}} z \left(1 - \frac{z}{h}\right)^2 Pr^{-1} \tag{117}$$

$$w_{\mathrm{s}} = \frac{u_*}{\phi_{\mathrm{M}}} \tag{118}$$

$$Pr = \frac{\phi_{\mathrm{H}}}{\phi_{\mathrm{M}}} \tag{119}$$

In the unstable outer layer the same expressions are used except that w_{s} and Pr are evaluated at $z = 0.1 \ h$ and that a counter gradient term is introduced in the heat and moisture equations:

$$\overline{w'\theta'} = K_H \left(\frac{\partial \theta}{\partial z} - \gamma_\theta \right) , \quad \overline{w'q'} = K_H \left(\frac{\partial q}{\partial z} - \gamma_q \right) ,$$ (120)

$$\gamma_\theta = C \frac{(\overline{w'\theta'})_0}{w_s h} , \quad \gamma_q = C \frac{(\overline{w'q'})_0}{w_s h} , \quad C \approx 8$$ (121)

where w_s is evaluated at the top of the surface layer ($z/h = 0.1$). If the stability functions obey free convection scaling, this closure will automatically provide the usual free convection velocity scale:

$$w_s = (u_*^3 + c_1 w_*^3)^{1/3} , \quad C = 8 ,$$ (122)

$$w_* = \left[\frac{g}{\theta_v} (\overline{w'\theta_v'})_0 h \right]^{1/3}$$ (123)

This closure is again an implicit closure in the sense that the expressions for the fluxes contain the fluxes. In practice this is solved by treating the surface layer exactly as is done in the local closure scheme. After the surface fluxes have been computed on the basis of the profiles at the previous time step, the exchange coefficients are specified.

The boundary layer height is an essential part of the parametrization in this scheme and has to be diagnosed. The following expression is used

$$h = \frac{Ri_c \{ U(h)^2 + V(h)^2 \}}{\left(\frac{g}{\theta_v} \right) \{ \theta_v(h) - \theta_{vs} \}}$$ (124)

where Ri_c is a critical Richardson number with a numerical value of about 0.5, θ_{vs} is a virtual temperature somewhere in the surface layer (e.g. 10 m) and θ_v (h) is the virtual potential temperature at the top of the boundary layer. For the convective boundary layer the surface temperature is augmented with the temperature excess that the thermals have with respect to their surroundings:

$$\theta_{vs} = \theta_v + C \frac{(\overline{w'\theta_v'})_0}{w_s}$$ (125)

One of the main advantages of this scheme is that it is extremely robust with respect to numerical stability. The explicit calculation of the diffusion coefficients in the local K-closure can introduce stability problems even if the solution method of the diffusion equation is fully implicit (Kalnay and Kanamitsu 1988; Girard and Delage 1990; Beljaars 1991). The K-profile method is much more stable as it does not allow for oscillations in the profile of exchange coefficients.

A second advantage is that the non-local aspects of this closure allow for the inclusion of entrainment in the scheme. However, in the formulation as proposed by Troen and Mahrt, the entrainment is highly dependent on the details of the numerical formulation and on the vertical resolution.

A disadvantage of the scheme is that it may be difficult to develop generalizations for cloudy and baroclinic boundary layers.

3.5 TKE-closure

The simplest "higher order" closure is the specification of the diffusion coefficients with a prognostic variable for the turbulence kinetic energy (TKE). Many different formulations have been proposed; most of them are "truncated" versions of full 2nd order closure schemes. A good overview of the different approximations is given by Mellor and Mellor and Yamada (1974). Implementations in the context of forecast models are discussed by Delage (1974), Miyakoda and Sirutis (1977), Manton (1983), Thierry and Lacarrerre (1983), Smith (1984) and Dtmenil (1987). An example of such a closure is the one proposed by Thierry and Lacarrerre (1983):

$$\frac{\mathrm{d}E}{\mathrm{d}t} = -\overline{u'w'}\frac{\partial U}{\partial t} - \overline{v'w'}\frac{\partial V}{\partial t} - \frac{g}{\rho_0}\overline{w'\rho'} - \frac{\partial}{\partial z}\left(\overline{E'w'} + \frac{\overline{p'w'}}{\rho}\right) - \varepsilon \ , \tag{126}$$

$$K_M = C_K l_K E^{1/2} \ , \quad K_H = \alpha_H K_M \ , \quad K_E = \alpha_E K_M \ , \tag{127}$$

$$\varepsilon = C_\varepsilon \frac{E^{3/2}}{l_\varepsilon} \tag{128}$$

$$\overline{E'w'} + \frac{\overline{p'w'}}{\rho} = -K_E \frac{\mathrm{d}E}{\mathrm{d}z} \tag{129}$$

$$\frac{1}{l_\varepsilon} = \frac{1}{kz} + \frac{C_{LE1}}{h} - \left(\frac{1}{kz} + \frac{C_{LE2}}{h}\right)m_1 m_2 + \frac{C_{LE5}}{l_s} \tag{130}$$

$$m_1 = 1/\left(1 + C_{LE3}\frac{h}{kz}\right)$$

$$m_2 = 1/\left(1 - C_{LE4}\frac{L}{h}\right) \quad \text{for } L < 0$$

$$= \quad 0 \quad \text{for } L > 0$$

$$\frac{1}{l_s} = 0 \quad \quad \text{locally unstable}$$

$$= \left[\left(\frac{g}{\theta}\right)\frac{\partial \theta}{\partial z}\right]^{1/2}E^{-1/2} \quad \text{locally stable}$$

$$C_\varepsilon = 0.125 \ , \quad C_K = 0.5 \ , \quad \alpha_H = 1 \ , \quad \alpha_E = 1 \ ,$$

$$C_{LE1} = 15 \ , \quad C_{LE2} = 5 \ , \quad C_{LE3} = 0.005 \ , \quad C_{LE4} = 1 \ , \quad C_{LE5} = 1.5 \ ,$$

$$\frac{1}{l_K} = \frac{1}{kz} + \frac{C_{LK1}}{h} - \left(\frac{1}{kz} + \frac{C_{LK2}}{h}\right)m'_1 m'_2 + \frac{C_{LK5}}{l_s} \tag{131}$$

$$m'_1 = 1 / \left(1 + C_{\text{LK3}} \frac{h}{kz} \right)$$

$$m'_2 = 1 / \left(1 - C_{\text{LK4}} \frac{L}{h} \right) \quad \text{for } L < 0$$

$$= 0 \quad \text{for } L > 0$$

$$C_{\text{LK1}} = 15 \ , \quad C_{\text{LK2}} = 11 \ , \quad C_{\text{LK3}} = 0.0025 \ , \quad C_{\text{LK4}} = 1 \ , \quad C_{\text{LK5}} = 3 \ .$$

The purpose of using the TKE equation is to have a prognostic equation for the turbulent velocity scale. A diagnostic equation is still needed for the length scales. More advanced models include an equation for the length scale (Mellor and Yamada 1982) or for the dissipation rate (Detering and Etling 1985, Beljaars et al. 1987, Duynkerke and Driedonks 1987). Here we limit to diagnostic length scales.

The background of the closure is relatively simple: we replace the unknown terms by dimensionally correct expressions in known model variables. The nature of the expressions is such that they represent the physics of the considered terms. Finally, adjustable constants are used to obtain a good fit with data. In the example above, the diffusion coefficients are chosen proportional to a turbulent velocity scale and a turbulent length scale. Both scales are supposed to represent the large transporting eddies, and the velocity scale is derived from the turbulent kinetic energy. The length scale is kz near the surface, proportional to h (boundary layer height) in neutral and unstable PBL's and limited by the Obukhov L in very stable flow. The diffusion of TKE is described in the same way as diffusion of momentum and heat i.e. down-gradient. Dissipation (transformation into heat by viscous forces) takes place at the smallest turbulent scales which are not modelled at all. The concept of energy cascade is used here which says that the energy loss at large scales is equal to the dissipation at small scales because no energy can be lost in the decay of turbulence from large scales to small scales. We therefore can model the dissipation in terms of large scale velocity and length scales. The amount of energy lost per unit of time on the cascade by the large eddies is proportional to E divide by the eddy turn-over-time $l / E^{1/2}$. This explains the parametrization of ε in terms of large eddy characteristics.

The TKE equation includes advection terms, but the turbulence terms have relatively short time scales which makes that the equation is in quasi-equilibrium most of the time. To simplify the equation, the advection terms can be neglected, whereas the time dependence can be retained simply as a technique to "iterate" the solution towards equilibrium. The main advantage of TKE closure is that it is the simplest closure with some non-local turbulence aspects. By means of the diffusion of turbulence from the production area in the mixed layer towards the capping inversion, this closure is capable of describing entrainment (although not necessarily quantitatively correct). Apart from this advantage it also enables the introduction of more advanced cloud parametrization schemes Smith 1984; Duynkerke and Driedonks 1987). It is disappointing, however, that experience so far at ECMWF has indicated that the scheme is more demanding on vertical resolution. From two different studies (Dtmenil 1987; Manton 1983) it was concluded that the TKE closure has hardly advantages over the simpler Louis (1979) closure with the resolution that is available in the PBL with the 19 level ECMWF model. A more fundamental problem with higher order closure schemes is that these schemes do not necessarily reproduce the surface layer similarity laws. These surface layer laws are always needed to specify the surface boundary condition at the lowest model level. This may result in an inconsistency between the lowest model layer and the layers aloft.

4. LIST OF SYMBOLS

$C_{\text{M}}, C_{\text{H}}, C_{\text{Q}}$ Transfer coefficients for momentum, heat and moisture

C_{MN}, C_{HN}, C_{QN}	Neutral transfer coefficients for momentum, heat and moisture
c_p	Specific heat at constant pressure
E	Turbulence kinetic energy
$\mathcal{E}$	Evaporation
f	Coriolis parameter
f	Functional dependence in general
g	Acceleration of gravity
h	Boundary layer height
F_M, F_H	Stability functions of Richardson number
H	Heat flux
k	Von Karman constant
K_M, K_H	Turbulent diffusion coefficients for momentum and heat
l	Turbulence length scale
L	Obukhov length
L_{vap}	Latent heat of vaporization
p	Pressure
p_0	Surface pressure
q	Specific humidity of water vapour
q_l	Liquid water specific humidity
q_t	Total water specific humidity
R	Gas constant for dry air
R_{vap}	Gas constant for water vapour
Ri	Richardson number
Ri_b	Bulk Richardson number
s	Dry static energy
s_l	Liquid water static energy
s_v	Virtual dry static energy
T	Temperature
U, V, W	Resolved or mean x, y and z velocities
$\mathbf{U}$	Horizontal vector (U, V)
U_G, V_G	Geostrophic wind components
u_*	Friction velocity
u, v, w	Total velocities in x, y and z directions

u', v', w'	Turbulent parts of the x, y and z velocities
w_e	Entrainment rate
w_L	Resolved vertical velocity
w_{*s}	Convective velocity scale in the surface layer
w_*	Convective velocity scale in the outer layer
x	Horizontal coordinate (usually west–east)
y	Horizontal coordinate (usually north–south)
z	Vertical coordinate (height above the surface)

ε	Dissipation of turbulence kinetic energy
φ_M, ϕ_H	Dimensionless wind and temperature gradients
γ	Potential temperature gradient above mixed layer
Ψ_M, Ψ_H	Dimensionless stability corrections in wind and temp. profiles
θ	Potential temperature
θ_l	Liquid water potential temperature
θ_v	Virtual potential temperature
θ_m	Mixed layer temperature
$\Delta\theta_m$	Temperature jump at the top of the mixed layer
θ_*	Turbulent temperature scale
λ	Asymptotic turbulence length scale
Λ	Local Obukhov length
σ	Standard deviation
τ	Turbulent stress
τ_0	Surface stress
τ_x, τ_y	Horizontal components of stress
τ_{x0}, τ_{y0}	Horizontal components of surface stress
ν	Kinematic viscosity of air
ρ	Density

REFERENCES

Beljaars, A.C.M., Walmsley, J.L. and Taylor, P.A. (1987): A mixed spectral finite difference model for neutrally stratified boundary-layer flow over roughness changes and topography, Bound.-Layer Meteor., 38, 273-303.

Beljaars, A.C.M. and Miller, M. (1991): The sensitivity of the ECMWF model to the parametrization of evaporation from the tropical oceans, ECMWF Technical Memo No. 170.

Beljaars, A.C.M. (1991): Numerical schemes for parametrizations, ECMWF seminar proceedings on: Numerical methods in atmospheric models Vol II, 1-42.

Beljaars, A.C.M. and Holtslag, A.A.M. (1991): On flux parametrization over land surfaces for atmospheric models, J. Appl. Meteor., 30, 327-341.

Blackadar, A.K. (1962): The vertical distribution of wind and turbulent exchange in a neutral atmosphere, J. Geoph. Res., 67, 3095-3102.

Brutsaert, W. (1982): Evaporation into the atmosphere, Reidel publishers.

Businger, J.A., Wyngaard, J.C., Izumi, Y. and Bradley, E.F. (1971): Flux-profile relationships in the atmospheric surface layer, J. Atmos. Sci., 28, 181-189.

Clarke, R.H. and Hess, G.D. (1974): Geostrophic departure and the functions A and B of Rossby-number theory, Bound.-Layer Meteor., 7, 267-287.

Deardorff, J.W. (1972): Parameterization of the planetary boundary layer for use in general circulation models, Month. Weath. Rev., 2, 93-106.

Delage, Y. (1974): A numerical study of the nocturnal atmospheric boundary layer, Quart. J. R. Meteor. Soc., 100, 351-364.

Detering, H.W. and Etling, D. (1985): Application of the E-eps turbulence closure model to the atmospheric boundary layer, Bound.-Layer Meteor., 33, 113-133.

Driedonks, A.G.M. and Tennekes, H. (1984): Entrainment effects in the well mixed atmospheric boundary layer, Bound.-Layer Meteor., 30, 75-105.

Dtmenil, L. (1987): Turbulence closure applied to the parameterization of vertical diffusion in the ECMWF model, ECMWF Technical Memo No. 132.

Duynkerke, P.G. and Driedonks, A.G.M. (1987): A model for the turbulent structure of the stratocumulus-topped atmospheric boundary layer, J. Atmos. Sci., 44, 43-64.

Dyer, A.J. (1974): A review of flux-profile relationships, Bound.-Layer Meteor., 7, 363-372. Haugen, D.A. (ed. 1973): Workshop on micro meteorology, Am. Meteor. Soc.

Garratt, J.R. and Francey, R.J. (1978): Bulk characteristics of heat transfer in the unstable, baroclinic atmospheric boundary layer, Bound.-Layer Meteor., 15, 399-421.

Girard, C. and Delage, Y. (1990): Stable schemes for the vertical diffusion in atmospheric circulation models, Moth. Weath. Rev., 118, 737-746.

Hicks, B.B. (1976): Wind profile relationships from the 'Wangara' experiments, Quart. J. Roy. Meteor. Soc., 102, 535-551.

Hogstrom, U. (1988): Non-dimensional wind and temperature profiles in the atmospheric surface layer: A re-evaluation, Bound.-Layer Meteor., 42, 55-78.

Holton, J.R. (1979): An introduction to dynamic meteorology, Academic Press.

Holtslag, A.A.M. (1984): Estimates of diabatic wind speed profiles from near-surface weather observations, Bound.-Layer Meteor., 29, 225-250.

Holtslag, A.A.M. and Nieuwstadt, F.T.M. (1986): Scaling the atmospheric boundary layer, Bound.-Layer Meteor., 36, 201-209.

Holtslag, A.A.M. and De Bruin, H.A.R. (1988): Applied modeling of the night-time surface energy balance over land, J. Appl. Meteor., 27, 689-704.

Holtslag, A.A.M., De Bruin, E.I.F. and Pan, H.L. (1990): A high resolution air mass transformation model for short-range weather forecasting, Month. Weath. Rev., 118, 1561-1575.

Kalnay, E. and Kanamitsu, M. (1988): Time schemes for strongly nonlinear damping equations, Month. Weath. Rev., 116, 1945-1958.

Kennedy, P.J. and Shapiro, M.A. (1980): Further encounters with clear air turbulence in research aircraft, J. Atmos. Sci., 37, 986-993.

Kim, J. and Mahrt, L. (1991): Turbulent mixing in the stable free atmosphere and the nocturnal boundary layer, submitted to Tellus.

Kondo, J., Kanechika, O. and Yasuda, N. (1978): Heat and momentum transfers under strong stability in the atmospheric surface layer, J.Atmos. Sci., 35, 1012-1021.

Large, W.G. and Pond, S. (1982): Sensible and latent heat flux measurements over the ocean, J. Phys. Oceanogr., 12, 464-482.

Louis, J.F. (1979): A parametric model of vertical eddy fluxes in the atmosphere, Bound.-Layer Meteor., 17, 187-202.

Louis, J.F., Tiedtke, M. and Geleyn, J.F. (1982): A short history of the operational PBL-parameterization at ECMWF, Workshop on boundary layer parameterization, November 1981, ECMWF, Reading, England.

Manton, M.J. (1983): On the parametrization of vertical diffusion in large-scale atmospheric models, Technical Rep. No. 39, ECMWF, Reading, UK.

Mason. P.J. (1985): On the parameterization of orographic drag, MET. O. 14, T.D.N. No. 177, Meteorological Office, Bracknell, UK.

Mason, P.J. (1988): The formation of areally-averaged roughness lengths, Quart. J. Roy. Meteor. Soc., 114, 399-420.

Mason, P.J. (1991): Boundary layer parametrization in heterogeneous terrain, In: ECMWF workshop proceedings on Fine-scale modelling and the development of parametrization schemes.

Mellor, G.L. and Yamada, T. (1974): A hierarchy of turbulence closure models for planetary boundary layers, J. Atmos. Sci., 31, 1791-1806.

Mellor, G.L. and Yamada, T. (1982): Development of a turbulence closure model for geophysical fluid problems, Rev. Geoph. Space Phys., 20, 851-875.

Miyakoda, K. and Sirutis, J. (1977): Comparative integration of global models with various parameterized processes of subgrid-scale vertical transports: Description of the parameterizations, Beitr. Phys. Atmos., 50, 445-487.

Monin, A.S. and Yaglom, A.M. (1971): Statistical fluid dynamics, Vol I, MIT press.

Monteith, J.L. (1981): Evaporation and surface temperature, Quart. J. Roy. Meteor. Soc., 107, 1-27.

Nieuwstadt, F.T.M. and Van Dop, H. (eds. 1982): Atmospheric turbulence and air pollution modelling, Reidel publishers.

Nieuwstadt, F.T.M. (1981): The steady-state height and resistance laws of the nocturnal boundary layer: Theory compared with Cabauw observations, Bound.-Layer Meteor., 20, 3-17.

Nieuwstadt, F.T.M. (1984): The turbulent structure of the stable, nocturnal boundary layer, J. Atmos. Sci., 41, 2202-2216.

Oke, T.R. (1978): Boundary layer climates, Halsted press.

Paulson, C.A. (1970): The mathematical representation of wind speed and temperature profiles in the unstable atmospheric surface layer, J. Appl. Meteor., 9, 857-861.

Smith, R.N.B. (1984): The representation of boundary layer turbulence in the mesoscale model: Part I - The scheme without changes of state, Met. Office 11, Tech. Note No. 186, Bracknell, UK.

Smith, R.N.B. (1984): The representation of boundary layer turbulence in the mesoscale model: Part II - The scheme with changes of state, Met. Office 11, Tech. Note No. 187, Bracknell, UK.

Smith, R.N.B. (1990): A scheme for predicting layer clouds and their water content in a general circulation model, Quart. J. Roy. Meteor. Soc., 116, 435-460.

Smith, S.D. (1988): Coefficients for sea surface wind stress, heat flux, and wind profiles as a function of wind speed and temperature, J. Geoph. Res., 93, 15467-15472.

Smith, S.D. (1989): Water vapor flux at the sea surface, Bound.-Layer Meteor., 47, 277-293.

Stull, R.B. (1988): An introduction to boundary layer meteorology, Kluwer publishers.

Taylor, P.A., Sykes, R.I. and Mason, P.J. (1989): On the parameterization of drag over small-scale topography in neutrally-stratified boundary-layer flow, Bound.-Layer Meteor., 48, 408-422.

Tennekes, H. and Lumley, J.L. (1972): A first course in turbulence, MIT press.

Tennekes, H. (1973): Similarity laws and scale relations in planetary boundary layers, in: Workshop on micrometeorology, ed. D.A. Haugen, AMS.

Thierry, G. and Lacarrerre, P. (1983): Improving the eddy kinetic energy model for planetary boundary layer description, Bound.-Layer Meteor., 25, 63-88.

Troen, I. and Mahrt, L. (1986): A simple model of the atmospheric boundary layer; sensitivity to surface evaporation, Bound.-Layer Meteor., 37, 129-148.

Ueda, H., Mitsumoto, S. and Komori, S. (1981): Buoyancy effects on the turbulent transport processes in the lower atmosphere, Quart. J. Roy.Meteor. Soc., 107, 561-578.

Van Der Hoven, I. (1957): Power spectrum of horizontal wind speed in the frequency range from 0.0007 to 900 cycles per hour, J. Meteor., 14, 160-164.

Van Wijk, A.J.M., Beljaars, A.C.M., Holtslag, A.A.M. and Turkenburg, W.C.(1990): Diabatic wind speed profiles in coastal regions: Comparison of an internal boundary layer model with observations, Bound.-Layer Meteor., 51, 49-75.

Van Wijk, A.J.M., Beljaars, A.C.M., Holtslag, A.A.M. and Turkenburg, W.C. (1990): Evaluation of stability corrections in wind speed profiles over the North-Sea, J. Wind Engin. Ind. Aerodyn., 33, 551-566.

Wieringa, J. (1986): Roughness-dependent geographical interpolation of surface wind speed averages, Quart. J. Roy. Meteor. Soc., 112, 867-889.

Wilson, M.F. and Hederson-Sellers, A. (1985): A global archive of land cover and soils data for use in general cir-

culation models, J. Clim., 5, 119-143.

Wood, N. and Mason, P.J. (1991): The influence of static stability on the effective roughness lengths for momentum and heat transfer, Quart. J. Roy. Meteor. Soc., in press.

Zilitinkevich, S.S. (1972): On the determination of the height of the Ekman boundary layer, Bound.-Layer Meteor., 3, 141-145.